Low-voltage grid assessment

Document ID:	SEMIAH-WP7-CSEM-Low-Voltage_Grid_Assessment
Document version:	1.0
Document status:	Submitted
Dissemination level:	PU
Deliverable number:	D7.1
Deliverable title:	Report on LV grid assessment
WP number:	WP7
Lead beneficiary:	CSEM
Main author(s):	Pierre-Jean Alet, Lionel Bally
Nature of deliverable:	R
Delivery date from Annex 1:	M10
Actual delivery date:	2015-07-07
Funding scheme / call:	STREP-FP7-ICT-2013-11
Project / GA number:	619560
Project full title:	Scalable Energy Management Infrastructure for Aggregation of Households
Project start date:	01/03/2014
Project duration:	36 months

Funded by the
European Union

This project has received funding from the European Union's Seventh Framework Programme for research, technological development and demonstration under grant agreement no 619560.

Executive Summary

The current quality of supply in European power networks is extremely high, with availability in excess of 99.99% and deviations from voltage quality standards rare events. This quality of supply is challenged by the increased use of distributed energy resources (DER) such as photovoltaic power generation, stationary storage, and demand response.

CSEM, EnAlpin and Agder Energi have investigated the potential impact of the SEMIAH concept on quality of supply at the low-voltage level through targeted literature review and measurements on operational networks. Two months of high-resolution power quality data have been acquired in feeders with high PV penetration in Norway and in Switzerland. Technical challenges were faced in this data acquisition as power quality measurement campaigns at low voltage are generally much shorter (one to four weeks) and only require the recording of data at ten-minute intervals.

Thanks to the sizing of the cables, voltage remained within a narrow range in the Swiss feeder. However, reverse power flows from the feeder to other feeders connected on the low-voltage side of the transformer have been frequently recorded. Extrapolation to summer time shows that reverse power flows to the medium-voltage side are likely. Large fluctuations in power factor on the feeder have also been correlated with net power injection from the PV system. In Norway, voltage dips and values of total harmonic distortion above standard limits have been observed, but none could be attributed to distributed energy resources.

Of the local issues observed or expected with high penetration of distributed power generation, overvoltage and reverse power flows come from the excess of generation with respects to local consumption. The SEMIAH concept could help in that respect by aligning as much as possible, at the household level and at the feeder level, local consumption with local production.

Demand response also carries its own risks for quality of supply. As communication infrastructures have a much lower reliability than electricity networks, the system must fall back to a safe behaviour in case of loss of communication. Aggregated demand response to wholesale market conditions reduces diversity in load profiles. This reduction in diversity can lead to infrastructure overload and rapid voltage fluctuations. It can be minimised by spreading response over time at the local level. This constraint is likely to increase the number of participants required to reach a desired volume of flexible power.

Abbreviations

ac	Alternating current
D	Deliverable
D-A-CH-CZ	Germany, Austria, Switzerland, and Czech Republic
dc	Direct current
DER	Distributed Energy Resources
DG	Distributed generation
DR	Demand response
DSO	Distribution system operator
EC	European Commission
ENS	Energy not supplied
FTP	File-transfer protocol
HF	High frequency
HV	High voltage
LV	Low voltage
LVR	Line voltage regulator
MV	Medium voltage
OLTC	On-load tap changer
PLC	Power-line communication
PV	Photovoltaic
PWM	Pulse-width modulation
RMS	Root mean square
SAIDI	System Average Interruption Duration Index
SAIFI	System Average Interruption Frequency Index
THD	Total harmonic distortion
TSO	Transmission system operator
VUF	Voltage unbalance factor
WP	Work Package
WT	Work Task

Contents

1 Introduction 7
2 Background analysis 7
2.1 Definitions of supply quality and grid stability 7
2.2 Evaluation of power quality 9
2.3 Preliminary risk assessment 11
2.3.1 Impact of distributed generation 11
2.3.2 Impact of demand response 17
2.3.3 Summary and quantification 18
3 Experimental approach 20
3.1 Characteristics of the test sites 20
3.1.1 EnAlpin test site (Visp, CH) 20
3.1.2 Agder Energi test site (Skarpnes, NO) 23
3.2 Handling of memory limitations 27
3.3 Measurement results 30
3.3.1 Active power: aggregate consumption from the MV grid and PV production 30
3.3.2 Maximum values of line loading and time of occurrence 32
3.3.3 Maximum values of rapid power variations 33
3.3.4 Measurement analysis 33
3.3.5 Skarpness 42
4 Impact of the SEMIAH concept on quality of supply 44
4.1 Possible improvements brought by SEMIAH 44
4.2 Possible detrimental effects 45
4.3 Integration of grid constraints in the SEMIAH concept 46
5 Conclusion 46
6 References 48
7 Change History 52

List of Figures

Figure 1: Reactive power billing scheme as applied to high-voltage customers by Swissgrid 14

Figure 2: Thermal loading of distribution feeders as a function of PV penetration level (reproduced from [23]) 15

Figure 3: Feeder losses throughout the day as a function of PV penetration level (reproduced from [23]) 15

Figure 4: Bird's view of the EnAlpin test site prior to construction 21

Figure 5: Map of the EnAlpin test site 22

Figure 6: Map of the Agder Energi test site 24

Figure 7: Connection diagram at the transformer substation (EnAlpin test site) 25

Figure 8: Connection diagram at the collective housing building (EnAlpin test site) 26

Figure 9: Connection diagram at the gym building with rooftop PV (EnAlpin test site) 26

Figure 10 - triggering the down sampling of recorded data 29

Figure 11: Normalised active power drawn from the MV grid and produced by the PV plant 31

Figure 12: Normalised active power drawn from the MV grid and produced by the PV plant over one day 31

Figure 13: Reactive power production at the gym building over one day 34

Figure 14: Reactive power profile at the gym building around the production peak 35

Figure 15: RMS voltage profile at the gym building over one day 36

Figure 16: Net active power injection from the gym building over one day 36

Figure 17: Short-term fluctuations in net active power injection from the gym building 37

Figure 18 - Current at the gym 38

Figure 19: Voltage profile at the gym building during a dip 38

Figure 20: Variations in power factor at the gym building around peak PV production 39

Figure 21: Active power consumption at the collective housing building 40

Figure 22: Reactive power consumption at the collective housing building 40

Figure 23: Power factor variations at the collective housing building 41

Figure 24: Power factor variations at the transformer end of the feeder 42

Figure 25: Active power consumption measured at the transformer end of the feeder 42

Figure 26: Maximum values of voltage THD measured on three phases over three months (Agder Energi test site) 43

Figure 27: Line-to-line voltage on three phases over 100 days (Agder Energi test site) 44

List of Tables

Table 1: Main voltage quality indices as per standard EN 50160 9

Table 2: Average number of voltage dips per MV measurement point (as per EN50160) in Italy in 2014; data obtained from [8]. 10

Table 3: Risk analysis for the deployment of distributed generation and demand-response schemes in low-voltage networks..... 19

Table 4: Physical characteristics of the lines in the EnAlpin test site 23

Table 5: Maximum values of line loading and time of occurrence (EnAlpin test site) 32

Table 6: Maximum difference in active power consumption between two time steps at 1 s acquisition rate (EnAlpin test site) 33

1 Introduction

Reliable, good quality power supply is currently taken for granted in Europe. This situation sets very high targets for any new technology to be implemented in power networks. As such, the SEMIAH concept must at least be compatible with maintaining quality of supply. The proposed architecture, with centralised optimisation and distributed action without horizontal communication, is challenging from this point of view as the central optimiser has little information on the environment of the households in which it operates.

However, quality of supply is also challenged by the deployment of distributed generation such as photovoltaic (PV) power generation. These challenges arise from the mismatch between production and demand on prosumers' premises [1]. By dealing with both aspects, the SEMIAH concept has the potential to safeguard quality of supply.

Since there is little prior experience on the impact of demand response mechanisms on the quality of supply, its investigation has been included at an early stage in the SEMIAH project, prior to the pilots or indeed most development. This assessment is therefore focused on evaluating the current situation of low-voltage distribution feeders with high levels of PV penetration, and on estimating potential risks and benefits arising from the SEMIAH concept.

The results reported here will be further investigated and generalised through modelling in SEMIAH's task 5.6, using data acquired in this work. They will then be integrated in the optimisation architecture to take into account physical constraints in the networks.

2 Background analysis

2.1 Definitions of supply quality and grid stability

The Council of European Energy Regulators (CEER) splits the quality of electricity supply into three components: continuity of supply, voltage quality, and commercial quality [2]. Commercial quality relates to the transactions between electricity companies and their customers such as sales, connection requests, or meter reading. This aspect is important in an unbundled environment with open competition; however, it is not related to technical aspects and therefore falls outside the scope of this work.

Indices used to monitor continuity of supply fall into three categories:

- Lost time, of which the most common is the System Average Interruption Duration Index (SAIDI), defined as the average amount of time per year that the supply to a customer is interrupted: $SAIDI = \frac{\sum_i N_i \times r_i}{N_T}$, where N_i is the number of customers interrupted by incident i, r_i is the restoration time for incident i, and N_T is the total number of customers in the system [3]. In 2010, values in Europe ranged from 17 minutes per year and customer (Denmark) to 386 minutes per year and customer (Poland). In the countries where the SEMIAH pilots are

planned, recent values are 66 minutes per year and customer (Norway, 2010) and 25 minutes per year and customer (Switzerland, 2013) [4]. This corresponds to an availability of 99.995%.

- Number of interruptions per year, of which the most common is the System Average Interruption Frequency Index (SAIFI), defined as: $SAIFI = \frac{\sum_i N_i}{N_T}$. For unplanned interruptions, the numbers in the EU range from 0.30 (Germany) to 4.32 (Portugal). Recent values in the countries where SEMIAH pilots are planned are 1.5 interruptions per year and customer (Norway, 2010) and 0.28 interruptions per year and customer (Switzerland, 2013). As a comparison, the average number of interruptions longer than 30 s for ADSL internet connections is between 0.4 and 0.9 per *day* and customer (UK, November 2014), out of which 0.1 to 0.4 last more than two minutes [5].
- Energy not supplied (ENS) is estimated based on interrupted power; this way, an interruption at time of high load has a higher impact on the value than one at time of low demand.

Voltage quality refers to deviations in shape and amplitude from the nominal voltage waveform. Such deviations include voltage harmonics, over- and under-voltage, and frequency deviations. The reference document in Europe for voltage quality is EN 50160. Its underlying concepts and requirements are described in [6]. The main requirements at the low-voltage level are:

Voltage disturbance	Voltage quality index	Limits
Supply voltage variations	U_{rms} (10-min average)	Within ±10% of nominal voltage for 95% of the week
		Within +10%/-15% of nominal voltage for 100% of the week
Flicker	$P_{lt} = \sqrt[3]{\sum_{i=1}^{12} \frac{P_{st,i}^3}{12}}$, where P_{st} is the short-term flicker severity, a quantification of the perception of flicker over a 10-min period such that if $P_{st} \geq 1$, at least 50% of observers will notice fluctuations in lighting	Below 1 for 95% of the week
Voltage unbalance	$\frac{U_{i,rms}}{U_{d,rms}}$, where $U_{i,rms}$ is the 10-min average RMS value of the inverse (negative) sequence component, and $U_{d,rms}$ is the 10-min average RMS value of the direct (positive) sequence component in the Fortescue transform	Between 0% and 2% for 95% of the week

Voltage disturbance	Voltage quality index	Limits
Harmonic voltage	10-min average of RMS value of harmonic voltage u_h	Within tabulated limits (between 0.5% and 6% of fundamental voltage u_1 depending on order h) for 95% of the week
	Total harmonic distortion $THD = \sqrt{\sum_{h=2}^{40} u_h^2}$	Below 8% of fundamental voltage u_1 for 100% of the week
Signals voltage (ripple control, power-line carrier signal, and mains marking signals)	3-s average value	Below frequency-dependent fraction of nominal voltage (from 9% at 100 Hz to 1% at 100 kHz) for 99% of the day

Table 1: Main voltage quality indices as per standard EN 50160

Most countries add to these common requirements either stricter limits or additional indices. For example, Norway limits the number of rapid (between 10 ms and 60 s) voltage variations larger than 3% of nominal voltage to 24 per day at low and medium voltage and 12 per day at high voltage level. In the DACHCZ area (Germany, Austria, Switzerland, and Czech Republic), rapid voltage variations of more than 6% are prohibited [7].

Finally, grid stability refers to the ability of the grid to maintain continuity of supply and voltage quality in case of perturbations. The main stability criterion consists in so-called (n-k) analyses, where the simultaneous loss of k lines is simulated.

2.2 Evaluation of power quality

Practices in power quality monitoring vary massively within Europe. The number of measuring units vary from 20 in Cyprus to more than 200'000 in France [2]. In the Czech Republic, Hungary, Slovenia, Norway, and Italy, continuous monitoring by the distribution systems operators (DSOs) is mandatory. It is generally done at the medium-voltage level in substations.

Measurements at the low-voltage level are generally done only on a temporary basis, either in a rotation of measurement equipment (at the substation) or following a complaint by a customer (at their supply terminal. Due to the formulation of power quality in EN 50160, the minimum duration of such temporary measurement campaigns is one week. The effective duration typically ranges between one and four weeks.

The measurement equipment must comply with standard EN 61000-4-30. Instant values of current and voltage are measured on each phase; the voltage quality indices, most of which are based on

10-min averages of RMS values or spectral analysis, are locally calculated and recorded. This approach keeps the amount of data to be stored or transmitted reasonable. Power quality measurement units come with operating software which can automatically generate standard power quality reports based on the measurements.

A limiting factor in power quality monitoring is the cost of power quality measurement units, which for low-voltage measurements ranges from 5'000 € to 10'000 €. Smart meters could provide additional information sources but their measurement capabilities are limited to voltage variations. In France, the smart meters should automatically report interruptions and voltage variations beyond tolerated limits to the DSO.

As a result, it is harder to get a global picture of voltage quality than continuity of supply. In Italy, RSE publishes aggregate data at high- and medium-voltage level [8]. In 2014, voltage levels remained well within the limits set by EN 50160 for all measurement points. At most one measurement point recorded deviations from ±7.5% from the nominal voltage for more than 5% of any given week. All values of total harmonic distortion were within standard limits. The most commonly recorded issue is flicker: several points each week recorded long-term flicker severity (P_{lt}) above 1% for more than 5% of the time. Voltage dips are the second category of relatively frequent deviations from voltage quality standard, as shown on Table 2. However, they are either shallow or short: the lowest value of residual voltage in dips longer than 5 s was 80% of nominal voltage.

	Dip duration [ms]		*Dip duration [s]*		
Residual voltage [%]	*[20, 200]*	*[200, 500]*	*[0.5, 1]*	*[1, 5]*	*[5, 60]*
[80, 90]	*72.5*	*5.2*	*0.5*	*0.5*	*0.4*
[70, 80]	*11.0*	*3.5*	*0.1*	*0.0*	*0.0*
[40, 70]	*14.2*	*3.9*	*0.3*	*0.2*	*0.0*
[5, 40]	*6.6*	*2.2*	*0.3*	*0.1*	*0.0*
[1, 5]	*0.4*	*0.2*	*0.0*	*0.0*	*0.0*

Table 2: Average number of voltage dips per MV measurement point (as per EN50160) in Italy in 2014; data obtained from [8].

In addition to actual measurements, network operators can evaluate the quality of supply and stability in their grid through modelling. The most commonly used calculation is the load-flow analysis, which estimates the voltage and current in different points of the network based on (assumed) consumption profiles and the impedance of network elements. Other analyses include harmonic propagation and fault analysis. The diversity of load profiles and the lack of actual data limits the accuracy of such calculations. It is particularly the case at the low-voltage level, where the influence of individual, unmeasured loads is most strongly felt. In most cases only the nominal

load with an assumed coincidence factor can be used or, at best, synthetic load profiles which underestimate short-term fluctuations.

2.3 Preliminary risk assessment

2.3.1 Impact of distributed generation

The impact of distributed power generation on voltage quality has been an active research topic for a few years. A central concept is that of “hosting capacity” i.e., the level of distributed power generation that can be added to a given network before any voltage quality issue arises [9], [10]. One of the most comprehensive studies on the integration of PV in the power system can be found in [11]. The Photovoltaic Power Systems programme of the International Energy Agency is also running a dedicated task [12], [13].

2.3.1.1 Overvoltage

Overvoltage is known to be the first issue to arise in most feeders with increasing levels of distributed power generation [11], [14], [15]. It has been shown to happen in residential UK feeders when installed capacity reaches 30% its maximum value[1] [16]. Indeed, voltage levels along electrical lines are affected by their reactance X,[2] their resistance R, and the levels of reactive and active power consumption by connected users. When $X \gg R$, voltage variations are mainly influenced by reactive power and for $X \ll R$, the influence of active power dominates. In high-voltage transmission networks, $X \gg R$. In low-voltage distribution grids, R/X is close to unity so both active and reactive power balances have an impact [17].

The design of existing networks assumed that users connected to the low-voltage level would be solely consumers of active power and therefore that voltage would decrease monotonously along feeders. The low-voltage side of MV/LV transformers is therefore generally set above the nominal value to guarantee that voltage will not fall below the lower limit of the acceptable range. With distributed generators injecting active power however, voltage along feeders can increase as well as decrease. As a result users connected towards the end of feeders risk experiencing voltage levels above the upper limit of the acceptable range. This risk is exacerbated when lines are long or have a small section.

2.3.1.2 Voltage fluctuations

Solar power generation fluctuates due to weather variations. Solar irradiance can vary by as much as 20% in 4 s [18] due to passing clouds. As photovoltaic generators have very little inertia, this variability in irradiance translates into rapid changes in active power injection. Due to the link

[1] Defined as the total capacity obtained if all households installed a 5 kW_p system.

[2] $X = 2 \cdot \pi \cdot f \cdot L$ with $f = 50\ [Hz]$ and $L\ [H/m]$ its inductance

between active power and voltage levels in low-voltage grids, this phenomenon gives rise to rapid voltage fluctuations [19].

However, these variations do not create flickering. Indeed, measurements show insignificant effect of PV generation on P_{st} values [20].

2.3.1.3 Frequency deviation

Frequency mainly depends on the balance between active power generation and consumption in the entire synchronised area. For the system to be stable, the frequency has to be kept very close to the nominal value of 50 Hz in Europe. Since distributed generators (wind, PV) are connected to the grid through static converters they do not provide any inertia to the system and therefore reduce its resilience against frequency deviations [21].

However, as a system-wide parameter maintaining frequency is the responsibility of the transmission system operators (TSOs), acting as balancing authorities. It is therefore out of the scope of this work, and is supposed to be guaranteed by the design of the markets of which aggregators running the SEMIAH concept will operate.

2.3.1.4 Phase unbalance

Small size units (i.e. a few kW peak) of distributed generation, for example PV installed on individual houses and connected to low-voltage grid are usually connected on a single phase. If a large number of single-phase PV generators are connected to the same phase, imbalance between phases may arise. The primary solution is to connect each new PV generator with a cyclic distribution among the three phases in order to balance the PV power injection. With several PV generators, improvement has been observed in the voltage profile, i.e. less difference among the magnitudes of V_a, V_b and V_c than when all PV generators were connected on the same phase [22]. The practical way to obtain improvement is to minimise a distribution factor[3] describing the distribution of the connected DG among the three phases.

Unfortunately, some approaches to mitigate overvoltage issues such as on-load tap changers and reactive power control can have a negative impact on voltage balance between phases [22]. Even three-phase connection of distributed generators is no guarantee to maintain balance between phases. Indeed, with existing topologies, the same power is injected on all three phases. If reactive power consumption is different on the different phases, unbalance will arise.

2.3.1.5 Frequent operation of voltage-control devices

Voltage fluctuations due to distributed generation lead to an increased use of regulation devices such as on-load tap changers (OLTC), line-voltage regulators, and voltage-controlled capacitor

[3] $f_D = \left|\frac{n_a}{n_{tot}} + a \cdot \frac{n_b}{n_{tot}} + a^2 \cdot \frac{n_c}{n_{tot}}\right|$, with $a = e^{j \cdot \frac{2\pi}{3}}$ and where $n_a, n_b and\ n_c$ are the respective numbers of DG units connected to phase a, b and c, and n_{tot} is their sum

banks. Their frequent switching leads to additional voltage step changes, switching transients, and fluctuations of reactive power flow. They also lead to faster ageing of the devices [23]. In addition, the fluctuations in PV power generation can happen on a shorter timescale than the characteristic operation time of these passive devices [24].

2.3.1.6 Reactive power supply

At present, reactive power supply is dealt with in the market for ancillary services [25]. Its pricing status is therefore different from active power. But it has been shown that operation and production costs depend on the amount of both active and reactive power. Indeed both influence the loading of the lines and the voltage, which are the main constraints of the grid (thermal limitation and voltage stability requirements) [26]. Moreover, reactive power flow wastes energy by increasing losses and limits the transmission capacity [27]. Therefore a change in market is proposed in several papers for the reactive power to be sold simultaneously with active power [25]. Rewards for producing or absorbing reactive power at some times should also be considered to increase the possibility to adjust reactive power [28]. Another solution is not to offer payment for reactive power capability, but to consider it as a requirement [27].

New DG may increase the need of the power system for reactive power depending on the location of the units. Alternatively it may decrease this need if the locations are well chosen and if the DG units provide reactive power supply. Concerning the possibility for PV inverters to vary their power factor, it should be noted that it is not economically desirable for the PV producer as reactive power is not paid as high as active power, and decreasing the power factor means producing less active power (apparent power is constant), which is an opportunity cost.

An example of contract for exchange of reactive power is the “2011 concept” of Swissgrid, the TSO in Switzerland. For distribution networks directly connected to the transport network, a fixed range of free reactive power has been introduced. DSOs and electricity users directly connected to the transmission network can choose to participate actively in maintaining the voltage in the transport network and be rewarded for doing so. On the other hand, reactive power will be billed if it is exchanged outside defined limits. The free zone for exchange of reactive power can be seen in grey on Figure 1. W_p is the active energy and W_Q the reactive energy. It can be observed that the latter varies with the amount of exchanged active power above a certain threshold. This variation corresponds to a constant power factor of 0.9 [29]. Reactive power used outside this zone is billed at a fixed rate.

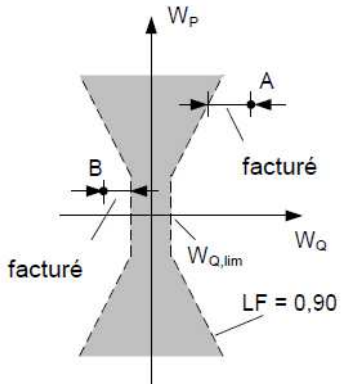

Figure 1: Reactive power billing scheme as applied to high-voltage customers by Swissgrid

2.3.1.7 Reverse power flows and loading of lines

PV generation can improve the utilization of lines as it decreases transmitted power (and losses) when PV penetration increase, in case of self-consumption i.e., when PV electricity is consumed at the point where it is generated. This is the case only until the amount of power produced by the PV corresponds to the local load, and transmitted power reaches a minimum as seen in Figure 2. Then, when DG increases above the local load, the surplus power has to be exported from households to neighbour feeders or to the transmission system. Such reverse power flows were not envisaged when designing current networks and can have a negative impact on protection devices and line-voltage regulators [23].

There is a limitation of current or apparent power to go through the cables. PV generation changes power flows and can lead to reaching these limitations. At the same time, when current in the cables increases, losses increase as they are equal to $R \cdot I^2$. Figure 3 shows the losses as PV penetration increases.

Even more than thermal line limitations, thermal ratings of transformers make them a bottleneck in the grid (overloaded station transformers limit the total power flowing through the grid). This can even be worsened by reverse power flows because limits are lower for on-load tap changer (OLTC) transformers, which impose an asymmetrical power flow limit [30]. This shows a trade-off between the advantages brought by OLTC in terms of voltage regulation and the issues it can create by limiting the reverse active and reactive power flow.

As reverse power flows occur, losses change and responsibilities for the change have to be determined to fairly adjust the billing of increased or decreased losses.

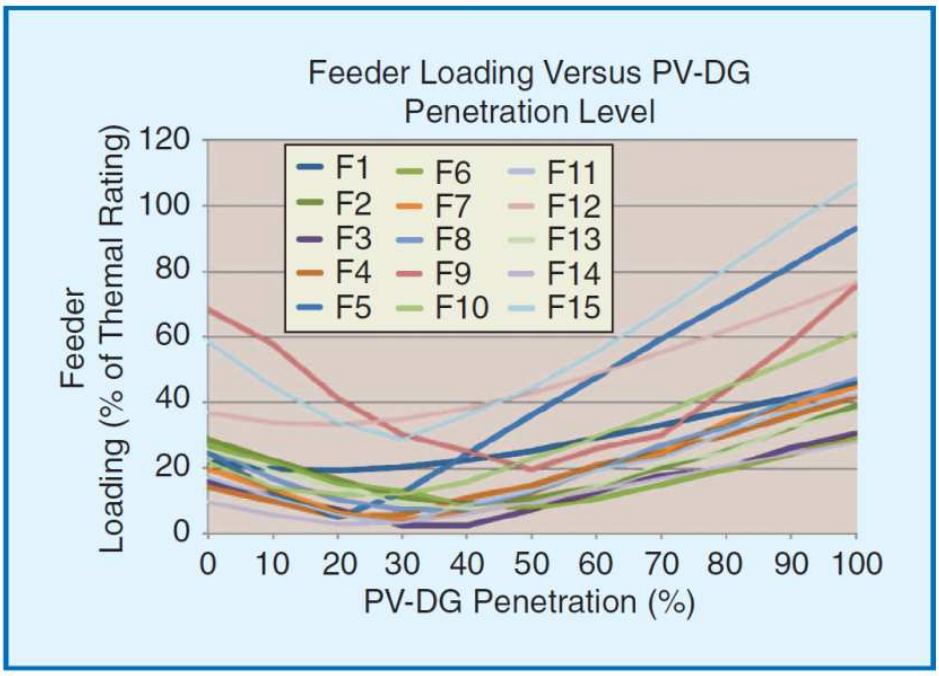

Figure 2: Thermal loading of distribution feeders as a function of PV penetration level (reproduced from [23])

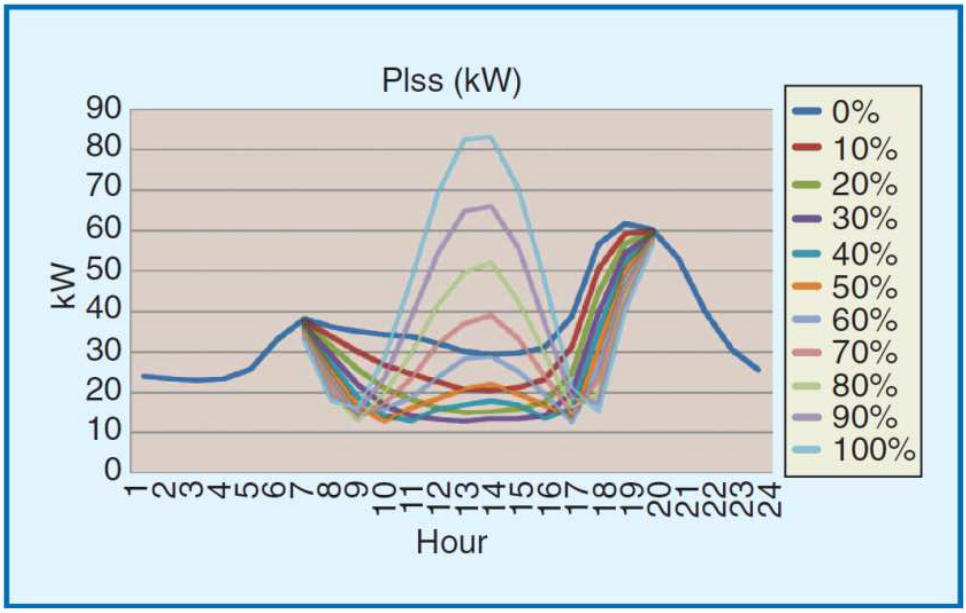

Figure 3: Feeder losses throughout the day as a function of PV penetration level (reproduced from [23])

2.3.1.8 Islanding

Both voltage and frequency regulations are created to stabilize the grid i.e., balance active and reactive power generation with the demand. The goal is that a maximum of generation units would be involved in the primary regulation, for example decreasing their generation of active power in case of over frequency. This can be problematic in case a part of the network is disconnected of the main grid. Indeed, under specific conditions, the disconnected part of the network could

stabilize itself thanks to the regulations put in place and get to a situation of unintentional islanding [31], [32].

This is not directly related to network stability, but it creates security issues and, if it happens, creates a need to resynchronize and therefore to recover stability.

Some solutions are proposed, like in [32], where several technical solutions are investigated by Enel Distribuzione. They mainly consist of protection devices to be installed in MV/LV substations and which can disconnect generators when they detect a situation that may cause an islanding event or remote control signals, for example power line communication (PLC), that can disconnect generators or change their settings. The challenge is how to detect such conditions preceding the islanding event with a high level of accuracy, and without giving wrong alerts.

2.3.1.9 Harmonics and HF

Inverters are the main source of harmonics. They are used in PV plants to transform dc into ac at the right frequency. Also, more and more heat pumps use inverter drives to reduce the inrush current and better control the motor, which is used for the compressor of the heat pump.

If one of the injected harmonics corresponds to a resonant frequency of the network, harmonic current impact may get amplified and create significant voltage distortion. This can potentially results in high total harmonic distortion (THD), even with relatively small amounts of harmonic generation [19]. Compared to distorted loads such as TVs or computers, the output current of PV inverters is a low distortion sinewave. It raises the issue that during periods of generation, only the fundamental current would be supplied by PV inverter to the load, whereas harmonics current must be supplied by the network. This could become a problem if the proportion of inverter-based generators continues to grow [20].

Concerning communication and measurement systems, the impact of harmonics can be divided in two parts. First, as most meters and sensors are traditionally designed to operate with an ideal sinewave, harmonics can create interferences [33]. Second, power-line communication (PLC) is based on superimposing a high-frequency signal on the mains sinewave. It is used for communications by some power meters and for the switching of some installations by the DSO (central command). Interference with this high-frequency signal by PV installations can result in a loss of communications and instabilities [34].

Certain harmonics can cause mechanical vibrations in machines, which can results in noise pollution or damage of the machine [33]. Another impact of harmonic distortion in power networks is due to extra heating losses ($R \cdot I^2$) in devices (e.g., feeder, transformers, motors, etc.) [33].

Some measurements on a grid with PV show high voltage distortion during daytime that can reach up to 1V [35]. As inverters usually use pulse-width modulation (PWM) to generate the output current, HF components around the PWM carrier signal frequency, typically between 15 and 20 kHz, and its multiples can be observed [35]. Some measurements of harmonics show emission from PV inverters is relatively low as no value higher than 5 % of the rated current were found [34].

2.3.2 Impact of demand response

The impact of demand-response schemes on stability and voltage quality has been relatively little explored.

A first conceivable risk is instability due to the feedback loop introduced between demand and wholesale market prices. Theoretical work has shown that application of real-time pricing to consumers leads indeed to increased volatility [36]. Demand response schemes based on aggregation i.e., the approach taken by SEMIAH, have been found better in terms of stability than ones based on prices to end users [37].

The second possible risk, loss of diversity, arises when participation in a given demand-response scheme increases. Load diversity is an important dimensioning factor for power networks. It is based on the observation that consumption patterns vary across electricity users. As a result, peak total demand on a network is lower than the sum of individual peak demand levels. The ratio between this sum and the total demand is called *coincidence factor*. It generally decreases with an increasing number of users. For electric water heaters, it is typically around 1/6 in Europe [38]. This observation enables great savings in infrastructure costs by dimensioning cables and transformers for a much lower load than the sum of nominal load of the users connected to the network.

Ripple control as used for example to control electric water heaters in peak/off-peak tariff structures is widely implemented in countries like France, Italy and Switzerland. As this approach is based on broadcast signals, it leads to a strong reduction in diversity and spikes in power demand. In a transformer station in Switzerland whose maximum load is 6 MW, overloading by more than 1 MW has been observed due to an almost instant rise in demand by about 6 MW in response to a ripple control signal [39]. Probabilistic analysis has shown that the loss of diversity depends on the duration of the controlled interruption of demand: from a starting point of 0.32, the coincidence factor increases to 0.39 after a ten-minute interruption, 0.8 after a two-hour interruption, and 0.95 after a four-hour interruption. In the latter case, more than five hours are necessary to reach back the initial coincidence of 0.32 [40].

This rebound effect has two detrimental effects on the network: it leads to rapid voltage fluctuations potentially beyond acceptable values, and increase cable and transformer loading potentially beyond their maximum values. It is particularly strong in the case of temperature-controlled load such as air-conditioning units, heat pumps or water heaters [41]. Indeed, after long interruptions it is necessary to compensate for thermal losses that occurred in the period and deviations from the comfort set-point [42]. The rebound effect can be integrated in the load forecasting so that sufficient generation capacity is available to serve the additional load after a sudden decrease of DR incentive [43]. This solution however does not solve the local network issues. The workaround put in place in the case of ripple control is to spread signals over time to avoid simultaneously turning on all controlled devices [39], [44, p. 159]. More generally, several control strategies of thermal electric loads have been investigated to mitigate the rebound effect [45]. The strategy which leads to the lowest peak load after interruption is the one which maintains the user's comfort during the interruption as the SEMIAH concept intends to do. However, this approach also delivers the lowest reduction in power and energy demand. Spreading complete switch off of appliances

over time seems to give the best compromise between effectiveness of the response to a load-reduction signal and minimisation of the rebound load.

2.3.3 Summary and quantification

The expected risks for low-voltage grids from the deployment of distributed power generation and demand-response schemes are summarised on Table 3. These risks are listed as undesirable, observable events and qualified by their possible root causes and consequences. The probability of occurrence and the severity of the consequences are each quantified between 0 and 1. These figures are subjective evaluations based on published information; they should therefore be seen as rankings rather than measurable quantities. The highest severity is put on events which can directly threaten lives. The next range of severity values (between 0.6 and 0.8) corresponds to events whose consequences can include the simultaneous loss of supply for a group of customers. Then come events which can compromise the supply of single customers and lead to degradation of hardware components. A risk value is derived for each event as the product of the occurrence probability and the severity of the consequences. Finally, some basic design choices for SEMIAH (aggregator approach, control of power consumption only) mean that SEMIAH neither influences the occurrence nor is affected by the consequences of some undesirable events; this information is indicated in the last column.

Event	**Root cause**	**Probability**	**Consequences**	**Severity**	**Risk value**	**Relevant for SEMIAH**
Current levels above rating of transformers or lines	Rebound effect at the end of demand-response events, loss of diversity	0.9	Increased losses, tripping of protection, faster ageing of transformers	0.6	0.54	Yes
Reverse power flows	Active power injection from DG	0.6	Tripping of protection devices, exceeding operating limits of OLTC	0.8	0.48	Yes
Rapid fluctuations of total power demand	Feedback loop between demand and wholesale market price (real-time pricing)	0.7	System instability, increased reliance on peaking generation capacity	0.6	0.42	No
Overvoltage	Active power injection from DG, grid dimensioning	0.8	Malfunction/damage to end-user appliances	0.5	0.40	Yes
Current levels above rating of lines or transformers	Active and reactive power injection from DG	0.4	Increased losses, tripping of protection, faster ageing of transformers	0.6	0.24	Yes

Event	Root cause	Probability	Consequences	Severity	Risk value	Relevant for SEMIAH
Phase unbalance above 2%	Non-coordinated single-phase connection of PV systems; reactive power control by PV inverters	0.7	Over-current, heating, and reduced torque in three-phase induction motors	0.3	0.21	No
Rapid voltage fluctuations larger than 3% of nominal value	Variations in PV production due to passing clouds	0.5	Tripping of relays and sensitive electronic equipment, stalling of induction motors	0.4	0.20	Yes
Harmonic distortion in excess of standard limits	Switching of power electronics converters (PV inverters, variable frequency drives), possible network resonance	0.5	Increased losses, mechanical vibrations in rotating machines, interference with PLC	0.4	0.20	No
Rapid voltage fluctuations larger than 3% of nominal value	Simultaneous switching at the beginning or end of demand-response event	0.5	Tripping of relays and sensitive electronic equipment, stalling of induction motors	0.4	0.20	Yes
Unintentional islanding	Fault at MV or HV levels and stable balance between local production and consumption	0.1	Danger to operators dealing with fault; need for resynchronisation after fault clearing	1.0	0.10	No
Slow voltage variations	Variations in active power injection from DG	0.9	Faster ageing of voltage regulation devices, and transients due to their operation	0.1	0.09	Yes

Table 3: Risk analysis for the deployment of distributed generation and demand-response schemes in low-voltage networks

3 Experimental approach

3.1 Characteristics of the test sites

Two test sites have been selected for voltage quality measurements. They are located in the networks where utilities partners to the project, EnAlpin and Agder Energi, operate. These utilities will also host pilot implementations of the SEMIAH system. However there is no guarantee that the pilots will be implemented on the same sites. The defining characteristic of the test sites is their high penetration of distributed power generation connected at the low-voltage level. In both cases, this power generation is from PV. As such, the measured networks differ from "typical" LV networks in Switzerland and even more in Norway, where PV penetration is very low.[5] Both are also recent networks whose dimensioning takes into account foreseen issues with distributed generation. In particular,

3.1.1 EnAlpin test site (Visp, CH)

The measurements in Visp were made at three points on a distribution feeder with high PV penetration, as at its end is connected a large photovoltaic plant of 145 kW_p placed on the roof of a gym.[6] The other two points are an apartment building and the beginning of the feeder, at the transformer station. A picture of the neighbourhood is shown on Figure 4 and a map of the electrical network is shown on Figure 5.

- The transformer station is called TS_Kleegärten
- The apartment building is called Sabbia
- The gym building with the solar plant is called Turnhalle

[5] About 10 MW_p of grid-connected PV in total

[6] Surface of 965 m^2, inclination of the roof is 11°-15° and is south-west oriented (60° of south)

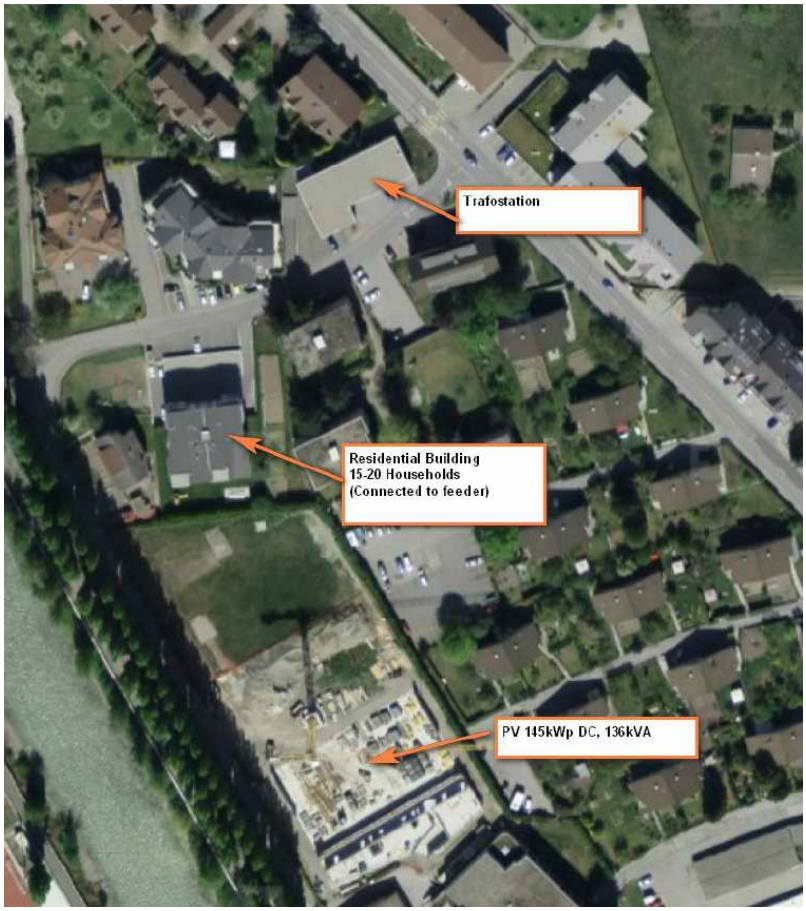

Figure 4: Bird's view of the EnAlpin test site prior to construction

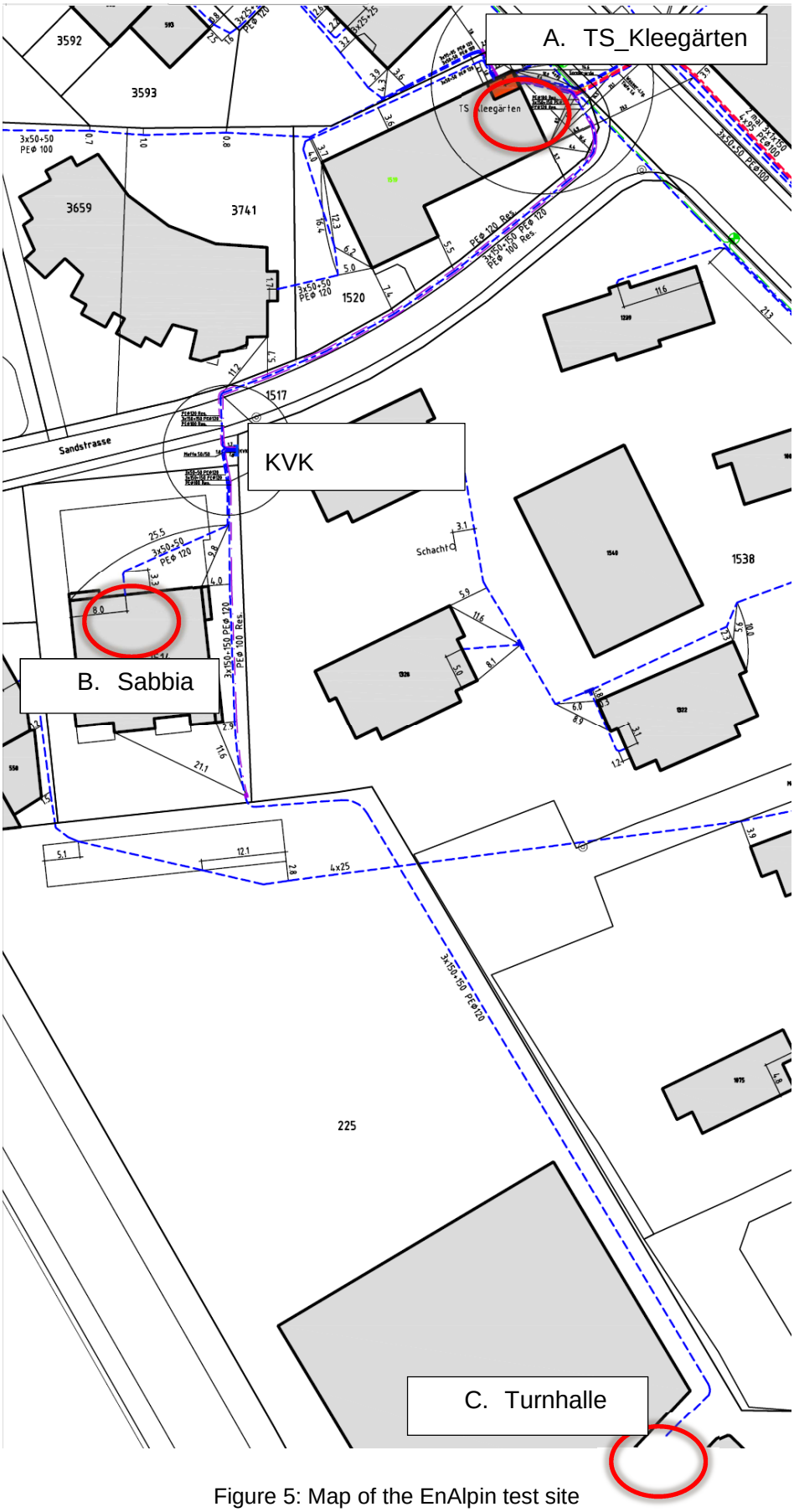

Figure 5: Map of the EnAlpin test site

Table 4: Physical characteristics of the lines in the EnAlpin test site

		line1	line2	line3
Start		TS_Klee	KVK Sandstrasse	KVK Sandstrasse
End		KVK Sandstrasse[7]	Turnhalle	Sabbia
Length [m]	Estimated on the plan	100	200	40
3x (3 phases)		150 mm^2	150 mm^2	50 mm^2
+ PEN	Protective earth & neutral	150 mm^2	150 mm^2	50 mm^2
PE internal diameter	Tube	120 mm	120 mm	120 mm
Material		copper	copper	copper
R[8] [Ω/km]	Positive sequence[9], both for conductors and neutral	0.122	0.122	0.379
X[10] [mH/km]		0.303	0.303	0.338
B[11] [μS/km]		144	144	97.3
Current ratings[12] [A]		342	342	175

3.1.2 Agder Energi test site (Skarpnes, NO)

Skarpnes is located along the coast in the southern part of Norway, around 260 km south of Oslo. Skarpnes housing estate is built by Skanska Norway, and is Scandinavia's first housing estate built with zero-house standards. Its geographical layout is shown on Figure 6. Construction work is still ongoing. In relation to the development, several parties are involved in a research project focusing

[7] Switchgear cabinet

[8] Table 7.5, copper, [48]

[9] Zero sequence values for cables were calculated as three times the value of positive sequence

[10] Table 7.7, column 8, [48]

[11] Table 7.9, column 8, [48]

[12] IEEE Table 4E1A, ref method B, 3 or 4 cables 3 phases a.c., http://www.csecables.com/technical-tables-useful-info/table-4e1a/

on how the buildings influence the quality in the LV distribution grid. Power quality measurements are in place at house number 6 and at the transformer substation. The network is a 400 V distribution grid which uses four-wire cables (three phases plus neutral). The section of the cables is 240 mm² between the substation and the cable cabinets, and is 25 mm² between the cable cabinets and the subscribers.

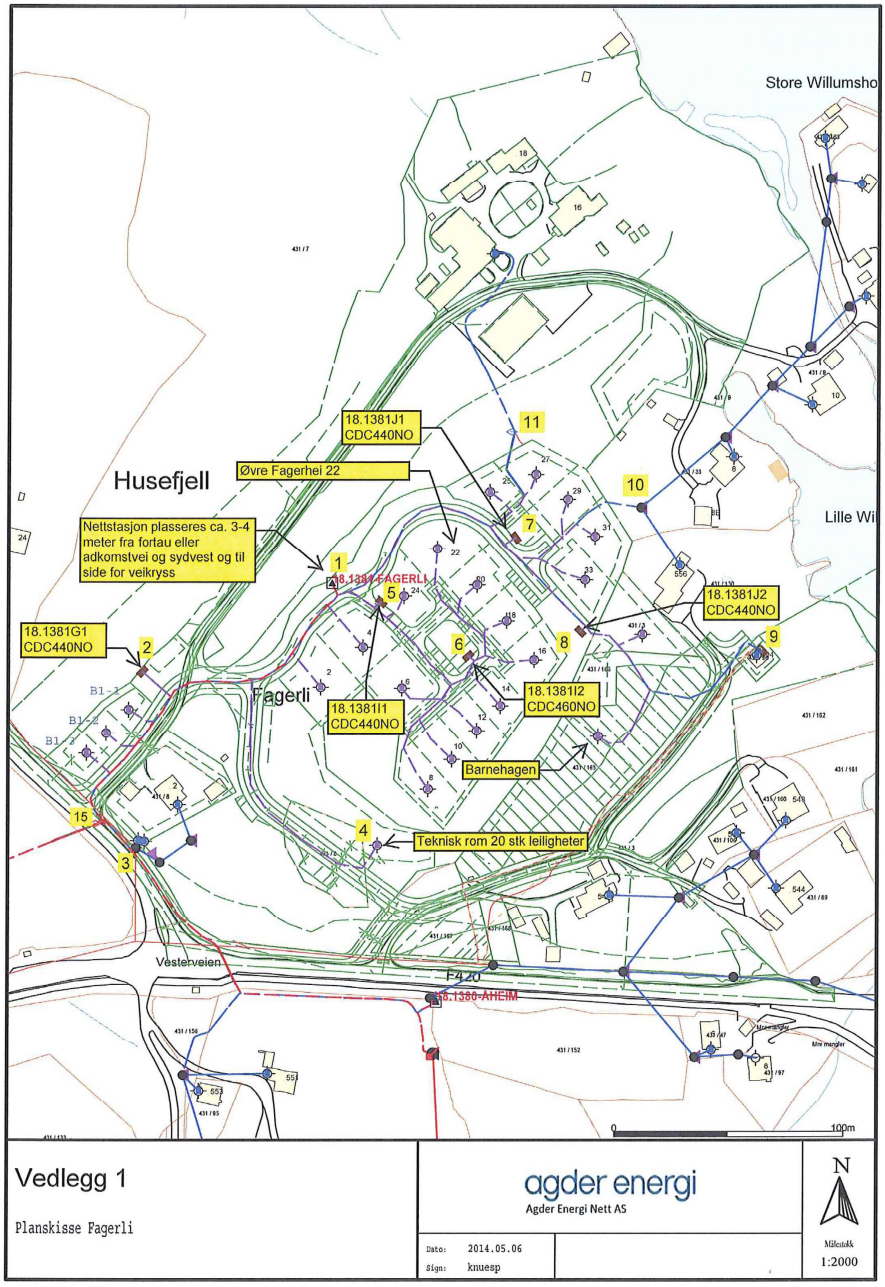

Figure 6: Map of the Agder Energi test site

The area is quite different from the selected pilot area in the SEMIAH project. While Skarpnes can be considered an urban area, the pilot area is a winter resort and hence sparsely populated most of the year (but highly populated during the skiing season). The rural characteristics make the grid less robust in the pilot area than at Skarpnes, and consequently more sensitive to loads that cause

power quality problems. Also, the houses in the pilot area are not zero-energy houses, nor do they have grid-connected PV systems. All these aspects highly influence the power quality in the grid. The results obtained based on the Skarpnes area cannot be used uncritically to describe the pilot area in SEMIAH. However, data from Skarpnes do provide a valuable general knowledge on challenges related to grid connected PV systems and power consuming equipment. This knowledge can further be brought into the development of the SEMIAH platform.Experimental protocol for measurements

In each feeder, measurements have been taken at three points: at the transformer substation (on the LV side), at the point of supply for one PV generator, and at another point of supply. Acquired data include: current (RMS), voltage (RMS), active power, reactive power, apparent power, power factor, THDI, THDU, individual harmonics (U, I from 1 to 50).

On the Adger Energi test site, Elspec G4400 power quality analysers [49] have been installed at the substation and on one zero-energy house with rooftop PV.

On the EnAlpin test site, three power analysers from HAAG, one Euro-Quant [50] and two Combi-Quant [51], have been used. Connection diagrams for each measurement point are shown in Figure 7, Figure 8 and Figure 9. They show the direction of the positive active power and power factor which depends on how current sensors were installed. Current is always shown positively.

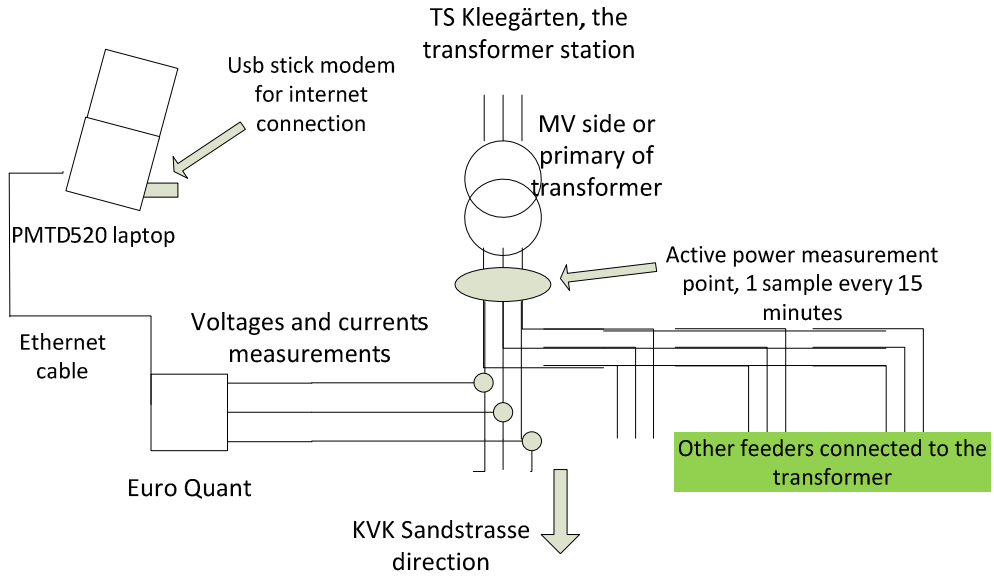

Figure 7: Connection diagram at the transformer substation (EnAlpin test site)

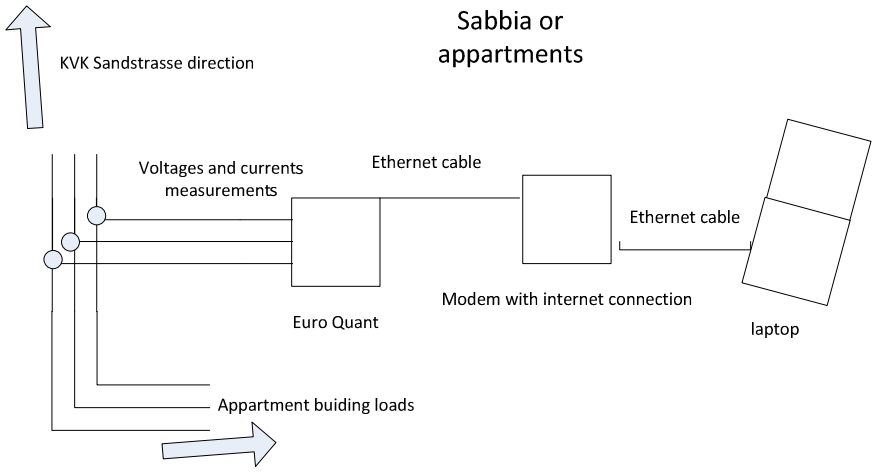

Figure 8: Connection diagram at the collective housing building (EnAlpin test site)

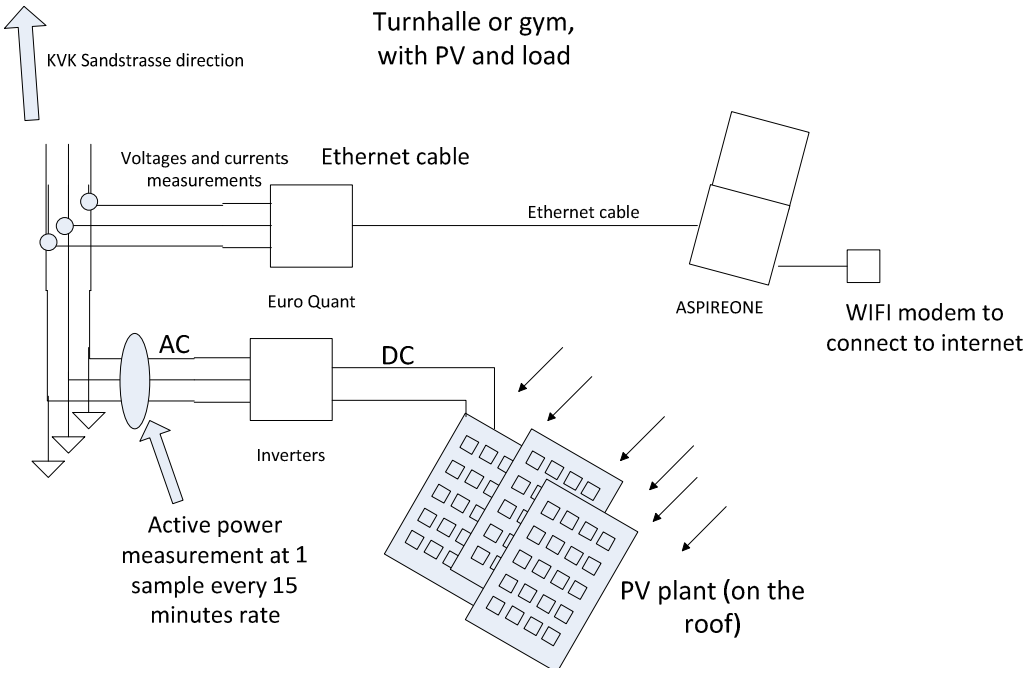

Figure 9: Connection diagram at the gym building with rooftop PV (EnAlpin test site)

The first measurement data were collected between the end of October and mid-November 2014 at a rate of 200 ms. No harmonics were measured. Voltage (U), current (I), active power (P), power factor (PF) and reactive power (Q) on three phases, as well as the sum on the three phases of active power (sumP) and reactive power (sumQ) were measured. Root mean square (RMS)

values[13] were recorded. For one point (other measurement devices were unable to do it), transient U was measured at 10 kHz.

For the two-month measurement campaign, the baseline sampling rate was one sample per second. For transient events, instant values of u(t) and i(t) were recorded at 10 kHz from a certain time before to a certain time after the event occurrence. This interval has to be limited as it uses a lot of memory.

Rate for flicker measurements was 1 sample every 10 minutes; rate for power-quality parameters such as THD and voltage unbalance factor, and other measurements of harmonics and interharmonics was 1 sample every minute.

Every measurement device was connected to a PC, which was connected to internet via 3G modem, as shown in Figure 7, Figure 8 and Figure 9. This allowed us to remotely control the installation. Also, in addition to the recording of the data on the PC, data was daily sent to CSEM FTP server for direct analysis of the data. Due to very low connection[14] e.g., in Sabbia where the modem is in a windowless basement, getting all the data directly on the FTP server was not possible every day at every points. All remaining data will be manually collected at the end of the two-month period.

3.2 Handling of memory limitations

Memory limitations were a major barrier. Measurement setups are normally used for short periods of times (i.e., one week) to investigate power quality complaints from customers.

Indeed, we found that internal memory of Combi-QUANT and Euro-QUANT was limited to storing about ten days of measurements at the initial 200 ms sampling period. Different ways to reduce memory use have been investigated. The main approach was to introduce a lower recording rate for most of the time, and to set triggers based on measured values to temporarily increase the recording rate in case of e.g., transients.

MATLAB/SIMULINK was used to simulate the measurement device and measured data at 200 ms rate was used as an input. These simulated devices had two possibilities of recording measured data. They record it at the rate is measured, i.e. 200 ms, and nothing change, or a higher rate is used and averaging of a certain number of 200 ms rate values is done[15].

[13] calculated on ten periods of the sinewave

[14] Connection speeds in the order of 100 kB/s proved to work. Speeds in the order of 10 kB/s were too slow for the connection to work. This can be due to the FTP server closing down excessively slow or weak connections.

[15] Note that for Combi-QUANT and Euro-Quant, the only available triggers signals are voltage and current. Trigger events can be parametrized for values higher or lower than a threshold. There is also a trigger for fast variation of voltage. Trigger can only start a transient measurement at instant values at a very high rate around 10 kHz, but not the averaging of RMS values. However, high rate measurements are very memory consuming.

For each measurement type, the trigger signal for low rate recording was defined to change when the difference between two consecutive measured values (200 ms rate data) was higher than a threshold. For that, consider the data vector of measured value for measurement type

$$meas,\ dataVec_{meas} = [val_i, \dots, val_{\frac{measured\ period}{200\ ms}}]$$

Equation 1: measured data vector definition

Then the difference between two consecutive samples is simply

$$diff_i = val_i - val_{i-1}$$

Equation 2

$$if \begin{cases} |diff| \leq threshold, & record\ at\ low\ rate \\ |diff| > threshold, & record\ at\ high\ rate \end{cases}$$

Equation 3: Definition of the trigger signal

This gives $diff\_compared\_to\_threshold = |diff| > threshold$ a Boolean signal defined as the trigger signal. Thus, when the condition changes, the recording rate should also change. However, some delay between the edge of $diff\_compared\_to\_threshold$ signal and the changing of rate was introduced.

The trigger signal is obtained in SIMULINK by comparing the absolute value of the difference between two consecutive samplings (using the delay function), as it can be seen on the left side of Figure 10. If the trigger signal becomes *true* (i.e. difference is higher than the threshold), the first *switch block* is on the upper position and its output is zero. This last one is compared to a constant in a block whose output is the Boolean value $input \leq num\_el\_to\_stab$. As $num\_el\_to\_stab = K = 5$ (K is the down sampling factor and value of 5 correspond to a down sampling of 1 second), input zero gives a true value which leads the second *switch block* to choose the normal sampled signal to output (*base_signal*). When the trigger signal becomes wrong, the first *switch block* adds 1 to the value compared to $num\_el\_to\_stab$ at each iteration and if the trigger signal keeps being wrong for more than $num\_el\_to\_stab$ iterations consecutively, the second *switch block* changes the recording rate to down sampling by a factor K until the trigger value of true occurs again. It can be seen at the bottom of the figure a block that computes the moving average of K samples at a time before down sampling. It resets at falling edge of threshold (when it goes from true to wrong, i.e. when it is needed to down sample after $num\_el\_to\_stab = K$ elements). The reset gives a good value of moving average when the output *compressed data* changes from *base_signal* to down sampled signal.

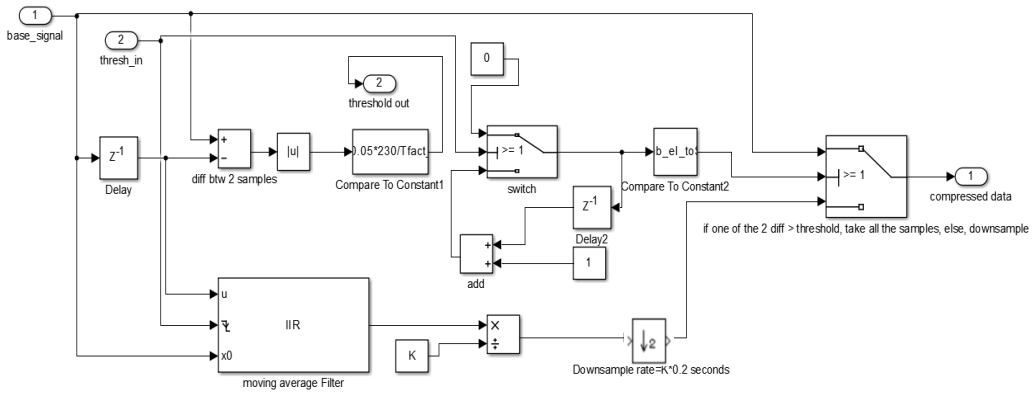

Figure 10 - triggering the down sampling of recorded data

For a better handling and processing of the data, both for further analysis and simulations, it was decided to always record all measurement types at the same rate. Therefore, it was decided that changing recording rate would be done identically for all the measurement types. This implies using only one trigger signal, which leads to choosing how to obtain it from the *number of measurement types* signals available. Comparing the data, it was observed that on one hand current *I*, active power *P* and apparent power *S* are strongly correlated, and on the other hand, reactive power *Q* and power factor *PF* are also correlated. Voltage *U* is not correlated with any other signals. This leads to the choice of three triggering signals, computed with *I1*, *U1* and *sumPF* trigger signals as total trigger signal

$$Trig = Trig_{I1} OR\ Trig_{U1}\ OR\ Trig_{sumPF}$$

Equation 4: trigger signal of mixed signal simulation

I was chosen rather than *P*, as it was observed that the rising edge of *I* usually come just before rising edge of *P*, and when high rate recording triggers, it can capture both edges if it keeps recording at high rate for long enough.

To quantify the loss of information, an error value is calculated as

$$error = \frac{\sum_i |u_i - \hat{u}_i|}{\sum_j \left(|u_j| - |\bar{u}|\right)}$$

Equation 5: error metric used

- $\hat{u}$ being the new signal $compressed\ data$
- u being the signal at 200 ms rate
- $\bar{u}$ being the average value of the 200 ms rate signal
- The sums are done over all the samples of the signals.

Different compressed signals, each one obtained with a different couple $(K, threshold)$ were compared based on their compression rate and their error. Error was computed as shown in Equation 5 and the compression rate was calculated as the ratio between the new number of sample over the base number of sample. A minimization problem was undertaken with the goal to

minimize the error (i.e., the loss of information), while respecting the constraint of the maximum compression rate (at most 10% of the amount of previous data[16]).

Due to limitations in the programming capabilities of the devices, it was finally decided to shift between recording of RMS data every second[17] and recording instant values based on trigger values.

Acquisition and handling of high-rate power quality measurements are very challenging. They require either remote access, which is difficult when measurements are done inside buildings, or large amounts of local storage. Supervisory capability is required to manage the setups for long measurement campaigns.

3.3 Measurement results

3.3.1 Active power: aggregate consumption from the MV grid and PV production

Figure 11 shows active power drawn from the MV grid and PV production along time in per unit (p.u.), i.e. calculated based on the nominal value. Nominal power of PV plant is taken as 145 kW (peak value) and nominal power of the transformer is taken as 400 kW (ratings are 400 kVA).

Measurements at the transformer station showed that reverse power flow never occurred at the transformer during the observed period. This means that the reverse power flow of the feeder studied here is flowing to other feeder on the LV grid and is never injected in medium voltage (MV) grid.

In summer, if PV production reaches up to 1 p.u., twice the maximum produced power than observed here will be injected in the feeder. In other words, 70 kW more could be injected in the feeder. As the active power taken from the MV grid when PV production reaches maximum is around 0.15 p.u. or 60 kW on some days, reverse power flow to the MV grid is expected to occur if peak power of PV plant is reached. That may happen in summer.

[16] To make sure memory would allow 2 month measured data continuously, the constraint value of 10% was found based on the assumptions that each sample takes the same weight of memory.

[17] Decision taken based on discussion with Mr. Jürg Pargätzi, PARMELTEC

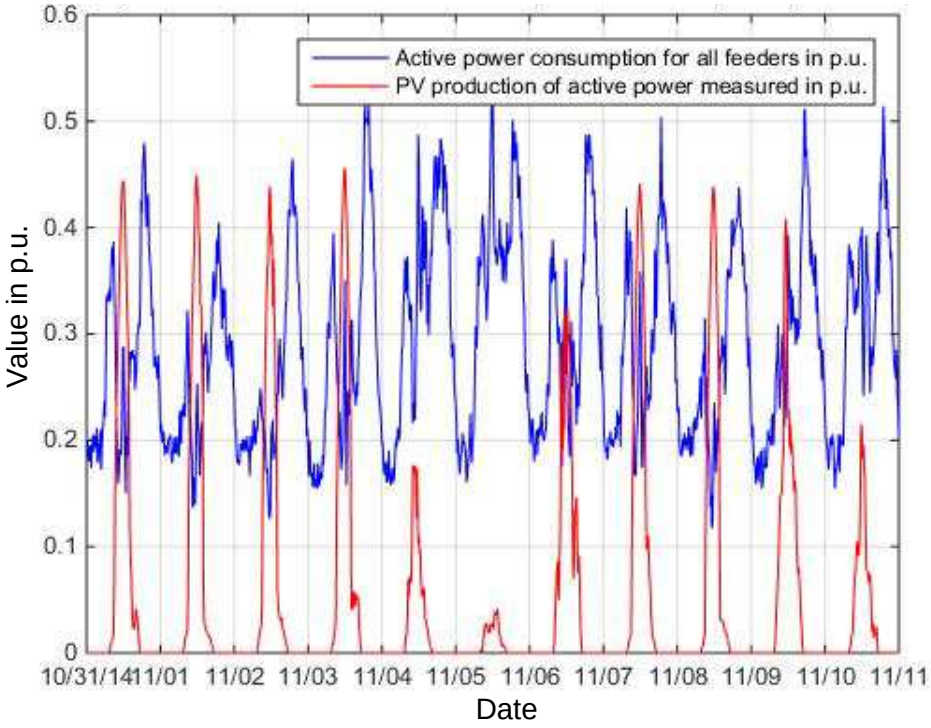

Figure 11: Normalised active power drawn from the MV grid and produced by the PV plant

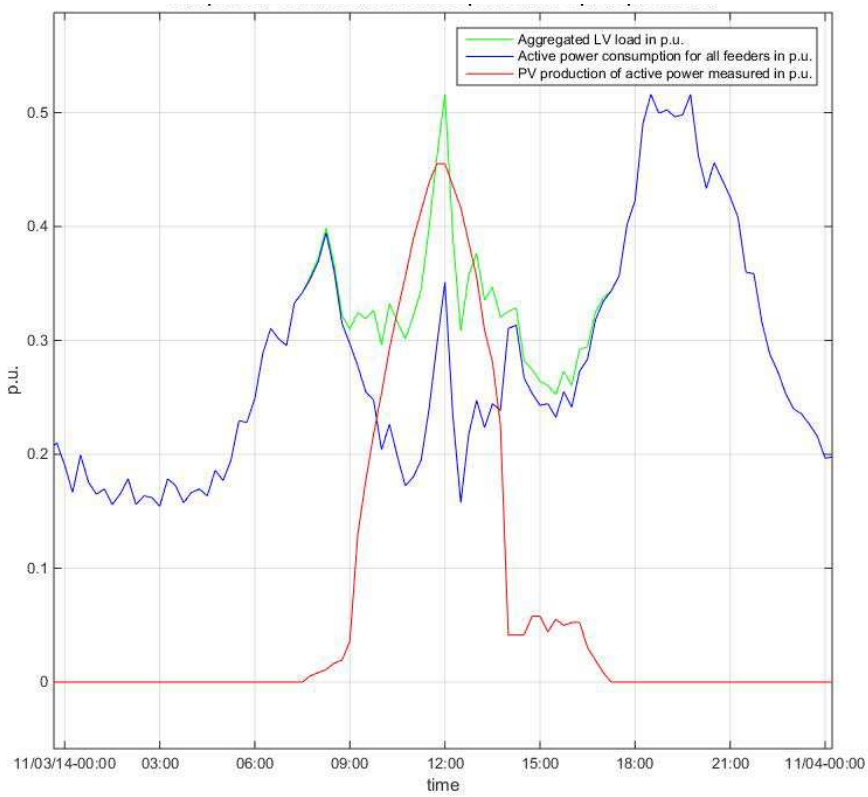

Figure 12: Normalised active power drawn from the MV grid and produced by the PV plant over one day

Figure 12 clearly shows that DR could make the active power profile taken from MV grid a lot flatter. Indeed, the evening peak load happens when no DG production is available. In the other side, except the peak happening around noon, the demand when PV production is at its highest is not as high as the 6:00-7:00 and the 18:00-20:00 peaks. The green curve, obtained by summing PV production with MV grid consumption, can be considered as aggregated load regarded the number of feeder it deserves.

3.3.2 Maximum values of line loading and time of occurrence

Place	Phase	Maximum values			Time of occurrence [dd.mm HH:MM:ss]		
		Current I [A]	Active power P [kW]	Reactive power Q [kVar]	I_{max}	P_{max}	Q_{max}
Klee	1	106	24	4.1	9.11 16:28:21	9.11 16:28:21	9.11 13:50:14
	2	92	21	4.2	8.11 19:58:03	8.11 19:51:19	4.11 16:09:03
	3	88	17	4.3	6.11 11:19:58	8.11 19:58:03	9.11 13:52:48
Sabbia	1	55	12	3.2	2.11 19:35:42	2.11 19:35:42	9.11 12:04:12
	2	45	10	2.7	6.11 18:35:30	6.11 18:35:30	9.11 11:52:02
	3	33	7.3	2.3	9.11 13:32:13	9.11 13:32:13	2.11 17:23:03
Turnhalle	1	93	16	3.3	6.11 11:24:45	9.11 16:47:57	1.11 12:25:04
	2	97	15	3.4	6.11 11:24:45	3.11 19:49:56	1.11 12:25:04
	3	88	14	3.2	6.11 11:24:45	9.11 16:56:46	8.11 2:00:46

Table 5: Maximum values of line loading and time of occurrence (EnAlpin test site)

As instant when current is maximum are the same than instant when active power is maximum in four situations (same phase and same location), and in a fifth one when the two instants are only seven minutes apart, it shows that I and P are correlated. Indeed, as voltage can be considered as constant, and if little reactive power is flowing in the grid, active power is directly depending on the current.

As the instant when P is at maximum in feeder is never the same than the instant when Q is at maximum in the same feeder, it gives information about the non-correlation of these two values.

As maximum values for Sabbia are smaller than for the two other places, it gives not a risk that a smaller cable is installed to connect the apartments to the feeder.

3.3.3 Maximum values of rapid power variations

Place	Phase	Active power difference ΔP [kW/second]	Time of occurrence [yyyy.mm.dd HH:MM:SS]
Klee	1	3.3	2014.11.05 16:19:25
	2	2.4	2014.11.06 07:05:53
	3	3.2	2014.11.05 12:59:24
Sabbia	1	2.7	2014.11.02 19:35:42
	2	2.5	2014.11.10 09:36:28
	3	2.5	2014.11.03 11:34:53
Turnhalle	1	2.6	2014.11.05 16:24:07
	2	2.1	2014.11.07 12:13:19
	3	1.9	2014.11.09 11:25:24

Table 6: Maximum difference in active power consumption between two time steps at 1 s acquisition rate (EnAlpin test site)

The impact of load profile modification by the demand response controller will be evaluated by modelling in SEMIAH's task 5.6.

3.3.4 Measurement analysis

This section presents the measurements obtained in Visp and comments are done to understand well the actual situation. First of all, be reminded that active power is called *P*, reactive power, *Q*, current, *I* and voltage *U*, with respective units of [*kW*], [*kVar]*, [*A]* and [*V*]. $P = U_{RMS} \cdot I_{RMS} \cdot PF$. Measurements were fully available for the three points of measurements for six entire days, between the 4th and the 9th of November 2014 included.

Q exchanged with the grid at the gym is shown in Figure 13 below. A repeated daily behaviour has been observed and looks like Figure 13. It can be seen that Q is always negative, which means it is consumed by the building, i.e. by the load, assuming PV inverters operate at unity PF. The amount of Q consumed is lower during the night and increases between 07:30, when PV begins to produce power, and 09:30, time when it reaches a maximum. As observed in Figure 16, this is the moment when PV production is becoming greater than consumption and gym begins to inject P into the feeder. Thus Q consumption exhibits a link with PV production. In [52] it was observed an increase of the net consumption of the reactive power at the distribution feeder. This is due to higher voltage (due to PV) and to the fact that PV provides only active power (PF = 1).

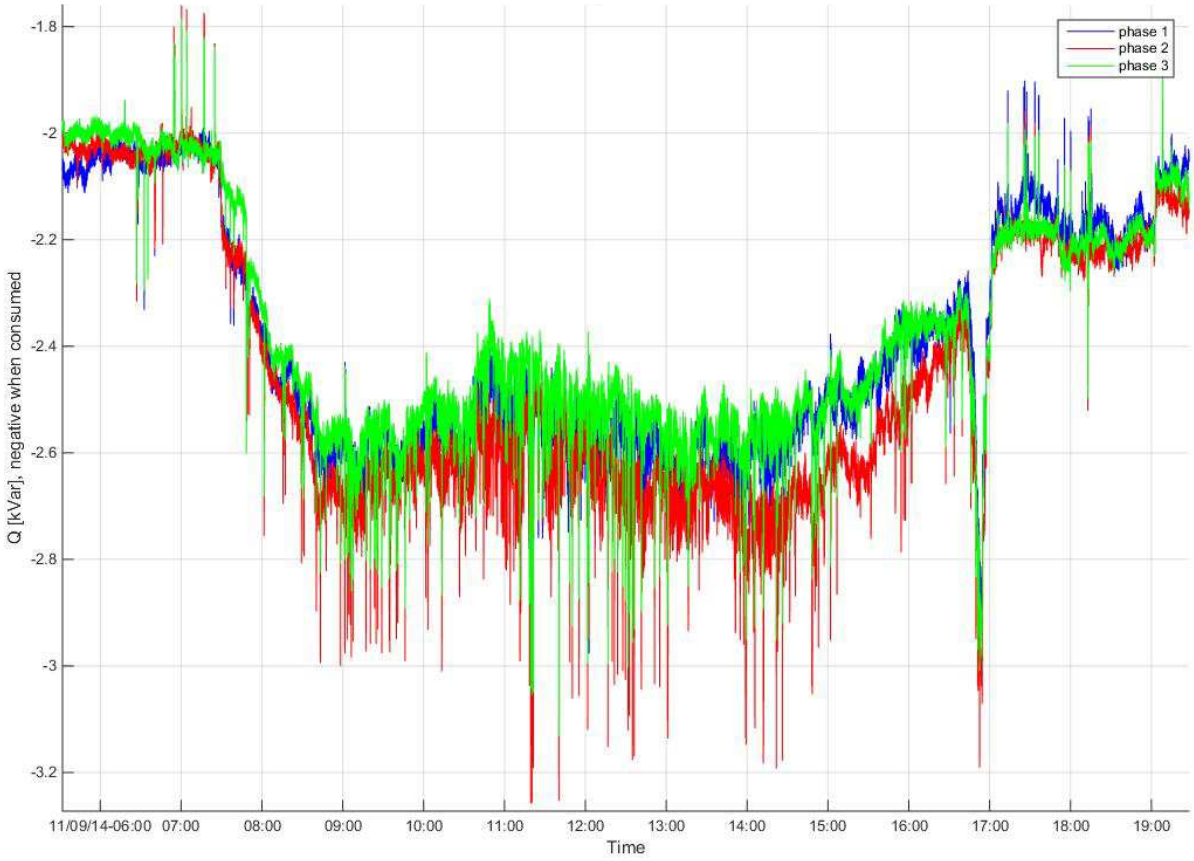

Figure 13: Reactive power production at the gym building over one day

A peak in Q consumption occurs just before 17:00 as shown in Figure 14. This is five to ten minutes before the PV production stops.

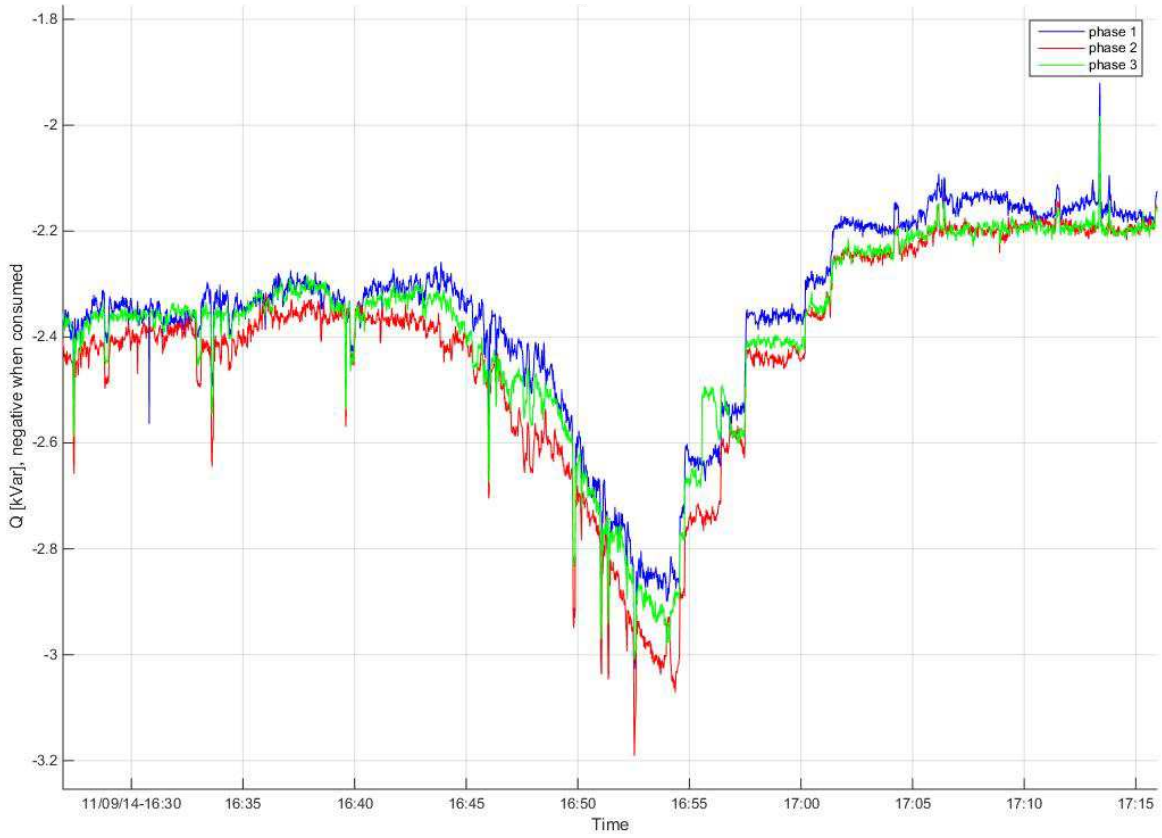

Figure 14: Reactive power profile at the gym building around the production peak

Voltage at the gym during one day is shown in Figure 15 a dip occurs at 07:00. Another minimum is reached at 19:00. The maximum value of 101 % of nominal voltage occurs at noon, when PV is producing maximum P. This shows the impact of PV on the voltage, due to reverse power flow. Indeed, net injection of active power increases the voltage at the end of the line as seen in section 2.3.1.1. This is why a positive correlation can be observed between voltage and injected power at the gym.

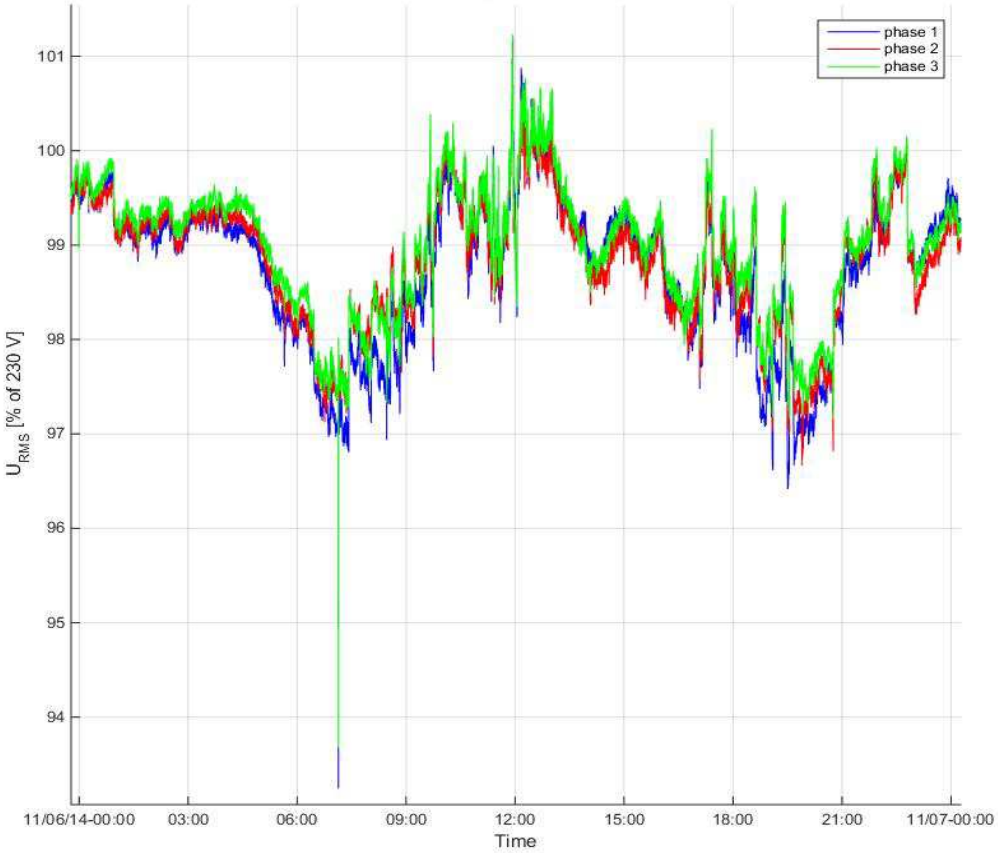

Figure 15: RMS voltage profile at the gym building over one day

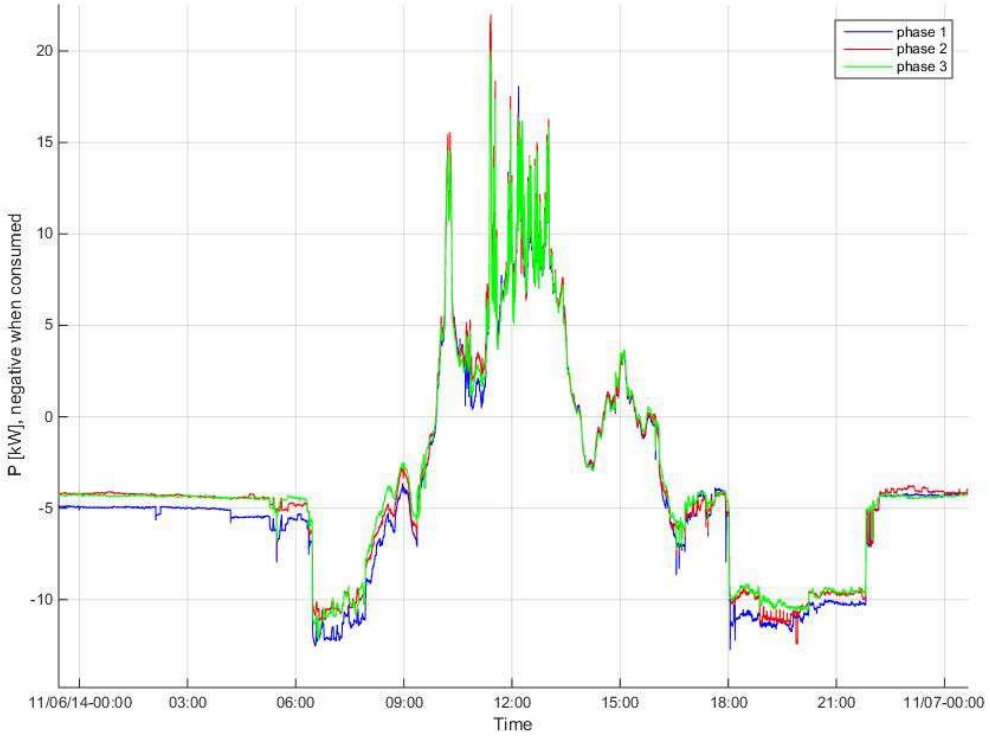

Figure 16: Net active power injection from the gym building over one day

P profile for one day is shown in Figure 16 and represents the typical daily profile observed in measurement sets, with some difference due to the level of irradiation. When there is not enough irradiation to meet at least self-consumption P is always negative. But when production is greater than consumption, P becomes positive, which means it is injected in the feeder. Fluctuation of injected active power is shown in Figure 17 and maximum rate of change around ten kW in less than one minute can be observed.

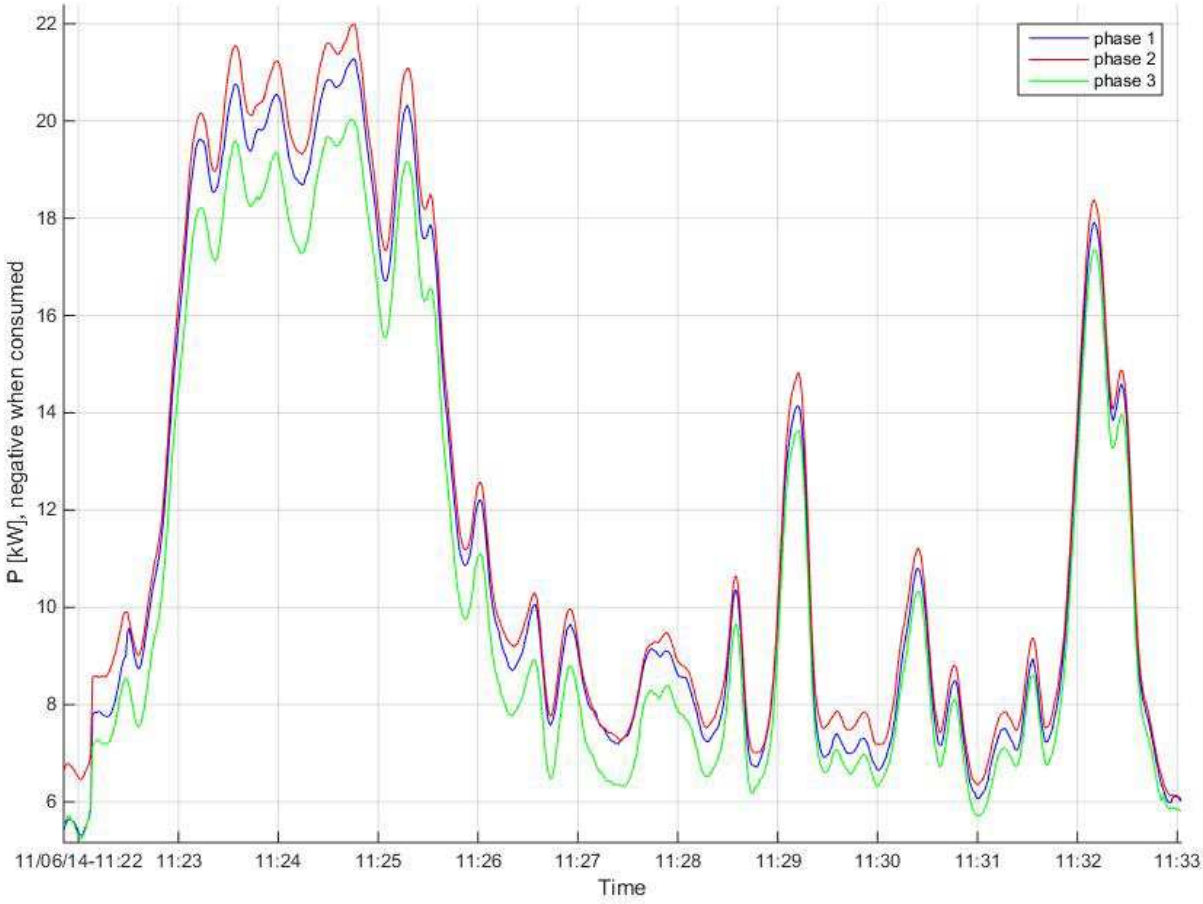

Figure 17: Short-term fluctuations in net active power injection from the gym building

When P exchanged with the feeder at the gym is close to zero, i.e. around 10:00, around 11:00 and during the period from 13:00 to 16:00, a lower value of the current can be observed in Figure 18. This minimum value of current never reaches zero, which is explained by the fact that even if there is no active power exchange, there is still reactive power exchanges with the grid.

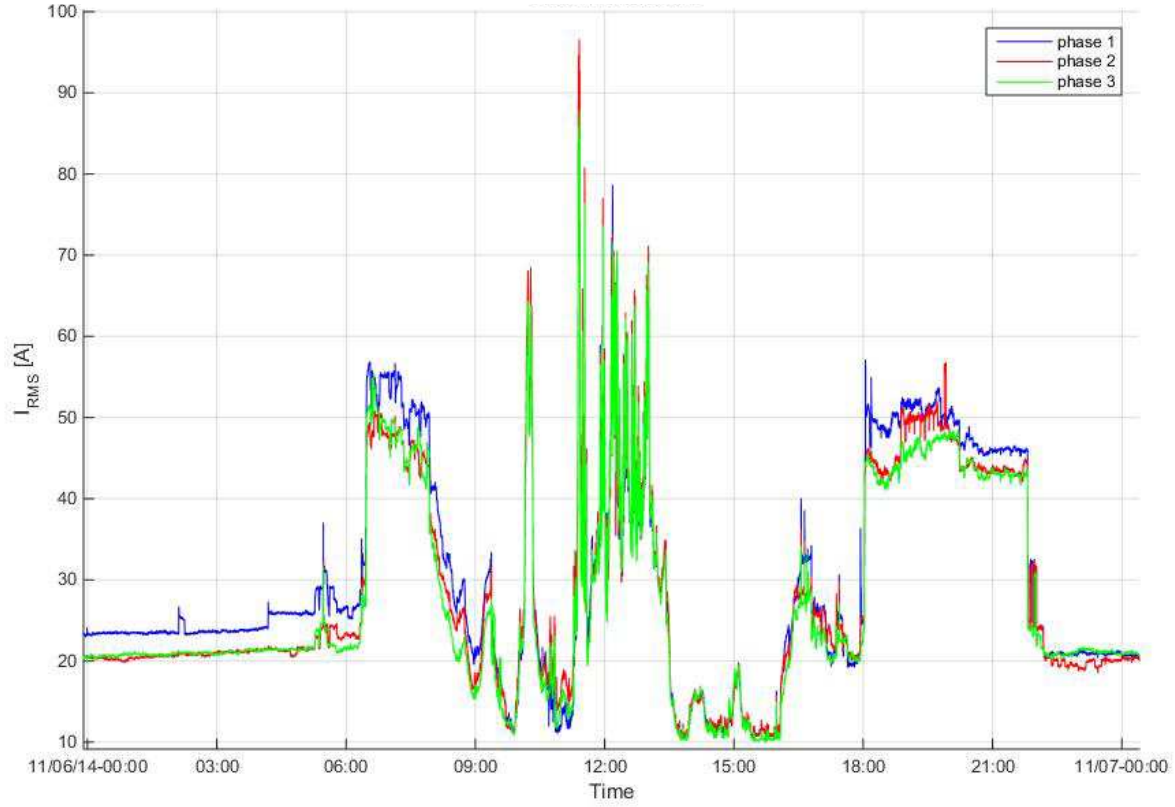

Figure 18 - Current at the gym

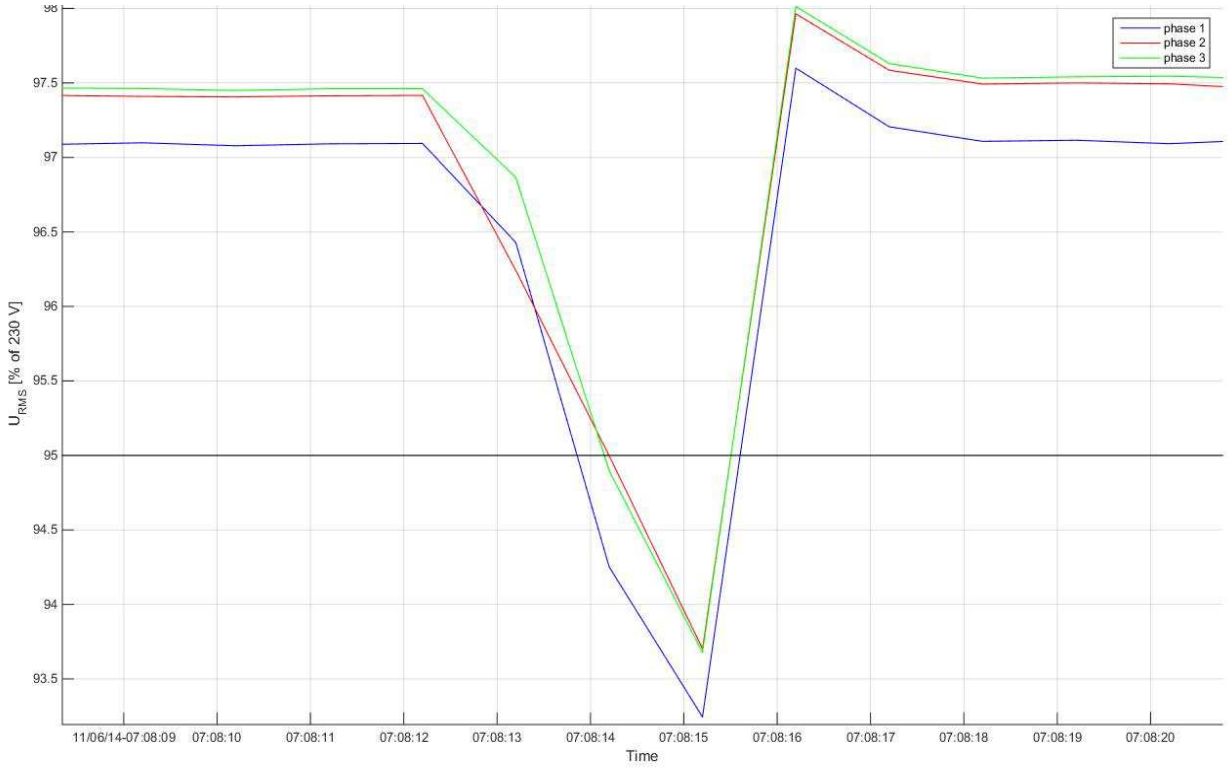

Figure 19: Voltage profile at the gym building during a dip

Figure 19 shows the only occurrence of voltage under 95% of the nominal voltage during the 6 days considered. This occurrence lasts for 1.6 seconds and voltage reaches down to 93% of nominal voltage. This is close to the limit of 90%, but is an isolated case. The margin between requirements for the voltage and the actual voltage band was higher than expected, due to over-dimensioning of the cables. As observed in Figure 15, variation between 97% and 101% of nominal voltage has been observed for most of the time.

No overvoltage on the line was measured even though reverse power flows were present from the feeder to the others. This seems to be due to the oversizing of the cable on which PV is installed as compared to other feeders. Simulation should be done to see the impact of having the same generation on a similarly sized cable as for other feeders

At the gym, active power almost never stays around zero. Either there is an important consumption, and power flow to the gym, either the production is higher than the consumption of the building thus showing a reverse power flow. The peak power of the solar power plant is so much higher than the average consumption that the case when PV produce just enough for self-consumption happens only on very cloudy days. But when it happens, fluctuations can be seen in the power factor as in the Figure 20 below.

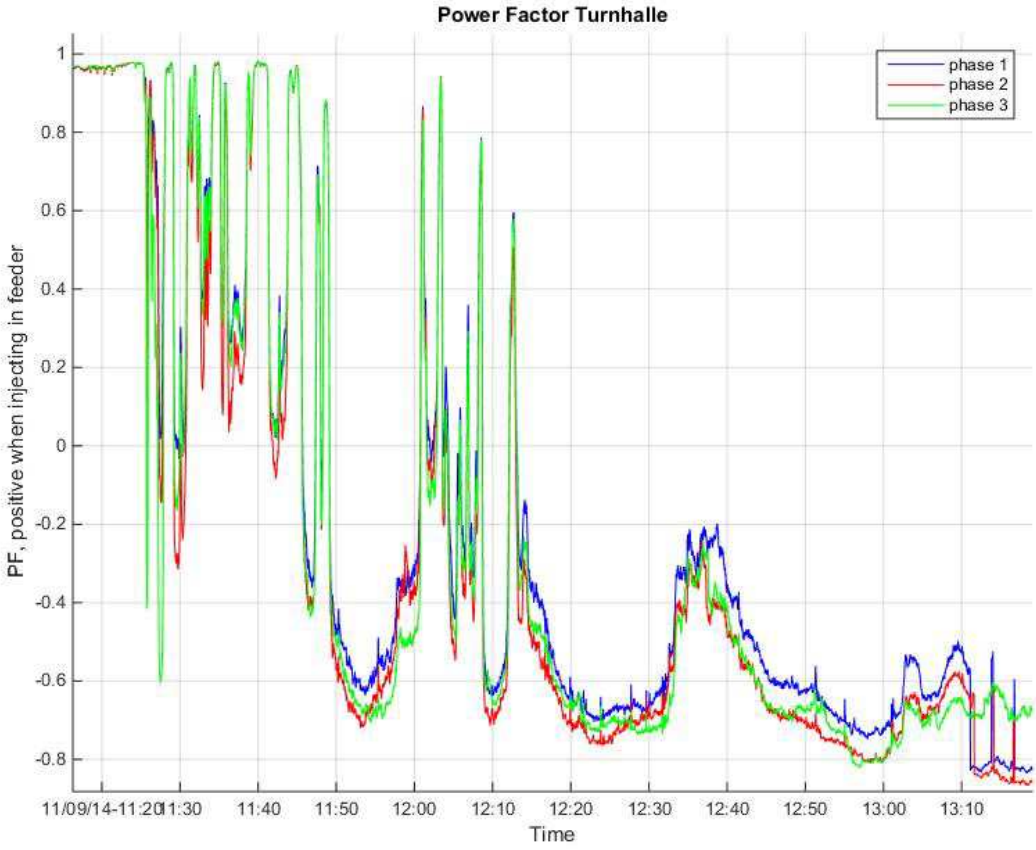

Figure 20: Variations in power factor at the gym building around peak PV production

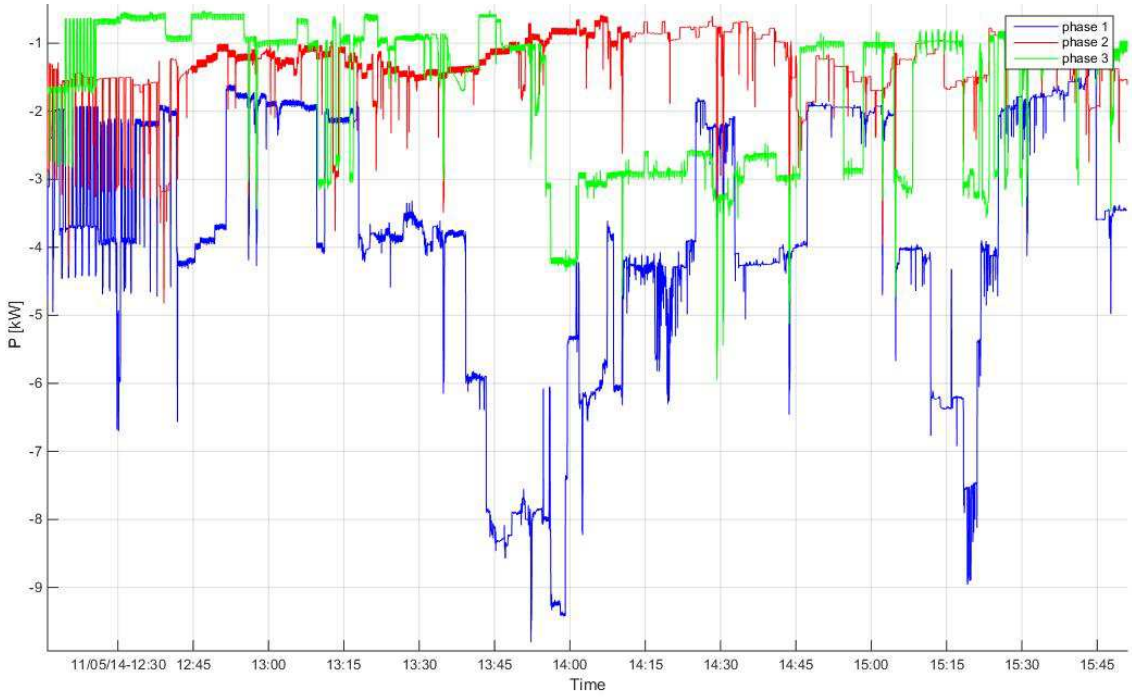

Figure 21: Active power consumption at the collective housing building

The active power consumption of the load at Sabbia, shown in Figure 21, is not the same on all phases. It means that different devices are using different phases and could create an unbalance.

The amount of Q consumed at Sabbia is smaller than the one consumed at the gym (Figure 21). However, PF is smaller and could be explained by the fact some loads are highly inductive.

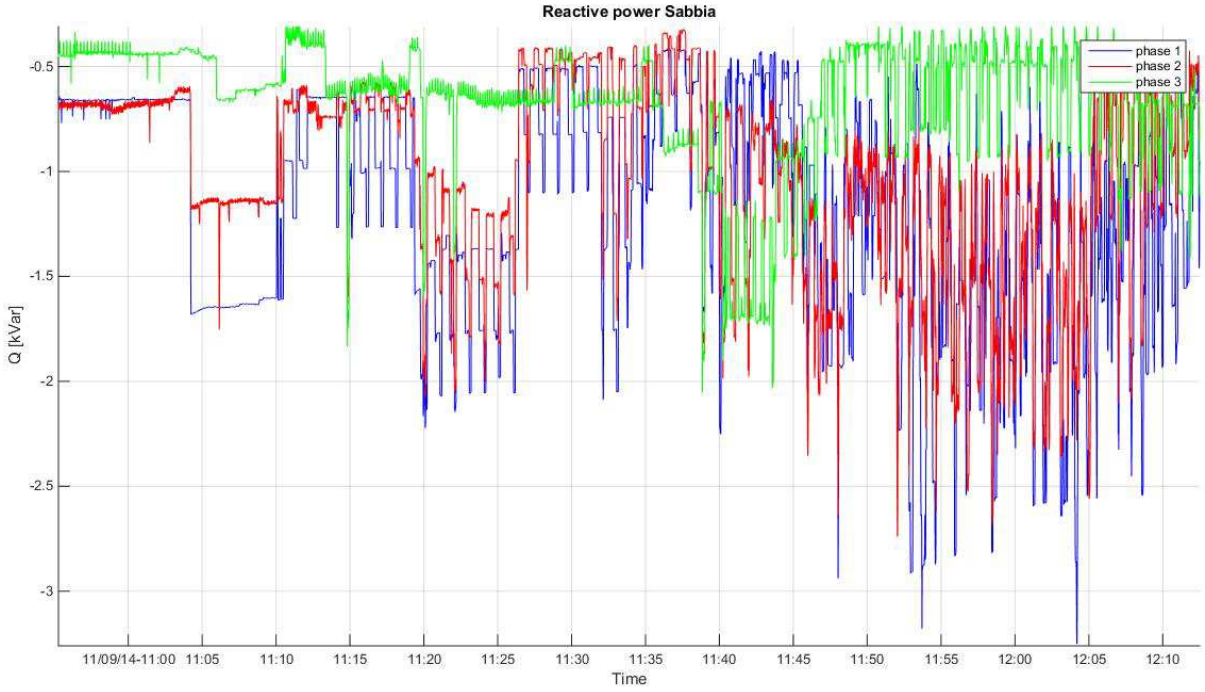

Figure 22: Reactive power consumption at the collective housing building

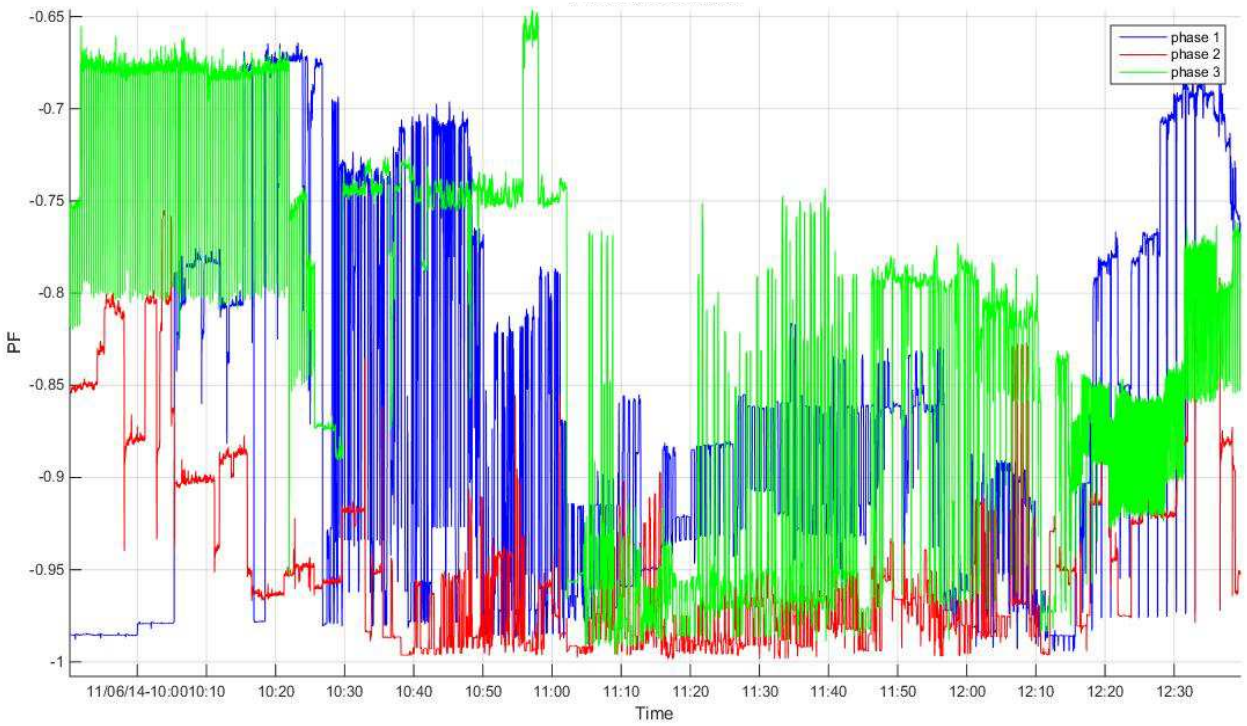

Figure 23: Power factor variations at the collective housing building

Finally, at the transformer, PF is positive (leading) during the night and when the feeder is not injecting power into the other feeders connected to the transformer. It can be seen on Figure 24 that when the power injected into the other feeder is close to zero, i.e. between 10:30 and 11.30 on the 6th of November (Figure 25), PF absolute value is not close to unity[18]. Unity power factor is the usual desired value as it is needed to maximize active power exchange rather than reactive power exchange. This low value of PF shows the need for locally supplied reactive power as discussed in section 2.3.1.6. Active power consumption measured at the transformer end of the feeder is given in Figure 25

[18] Similar results have been found in [53]. In fact, if there is a large amount of active power generated, which is used by the building, then the active power taken from the grid is smaller, with the same amount a reactive power taken from the grid, and utility experiences low power factor.

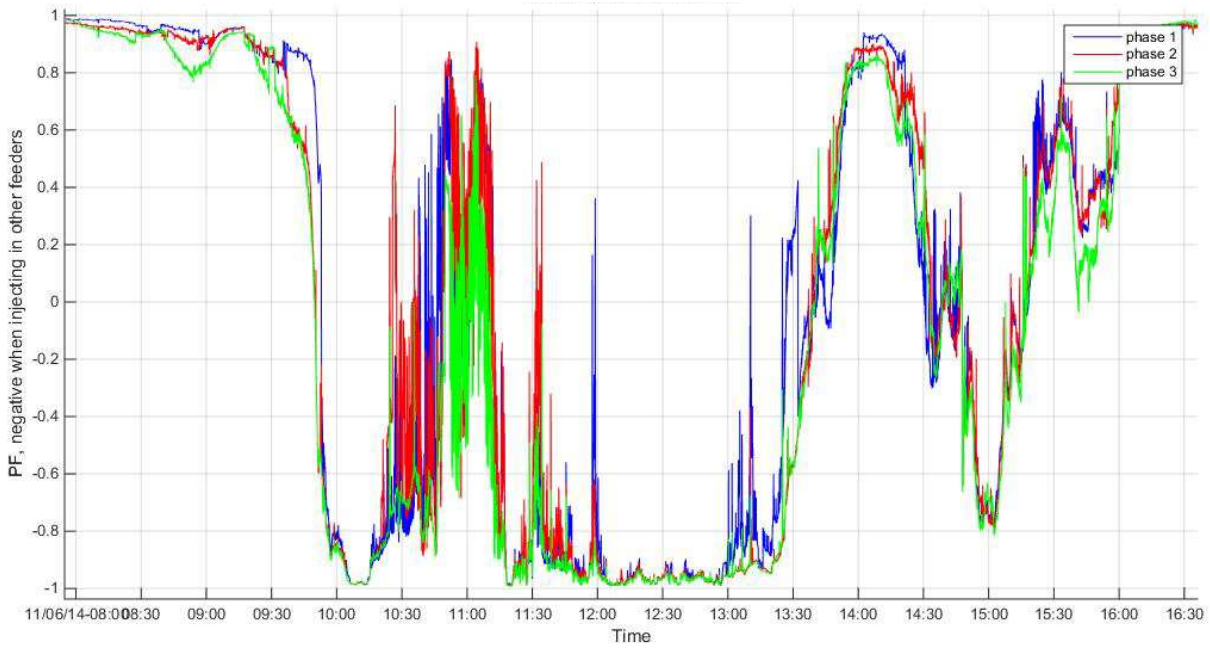

Figure 24: Power factor variations at the transformer end of the feeder

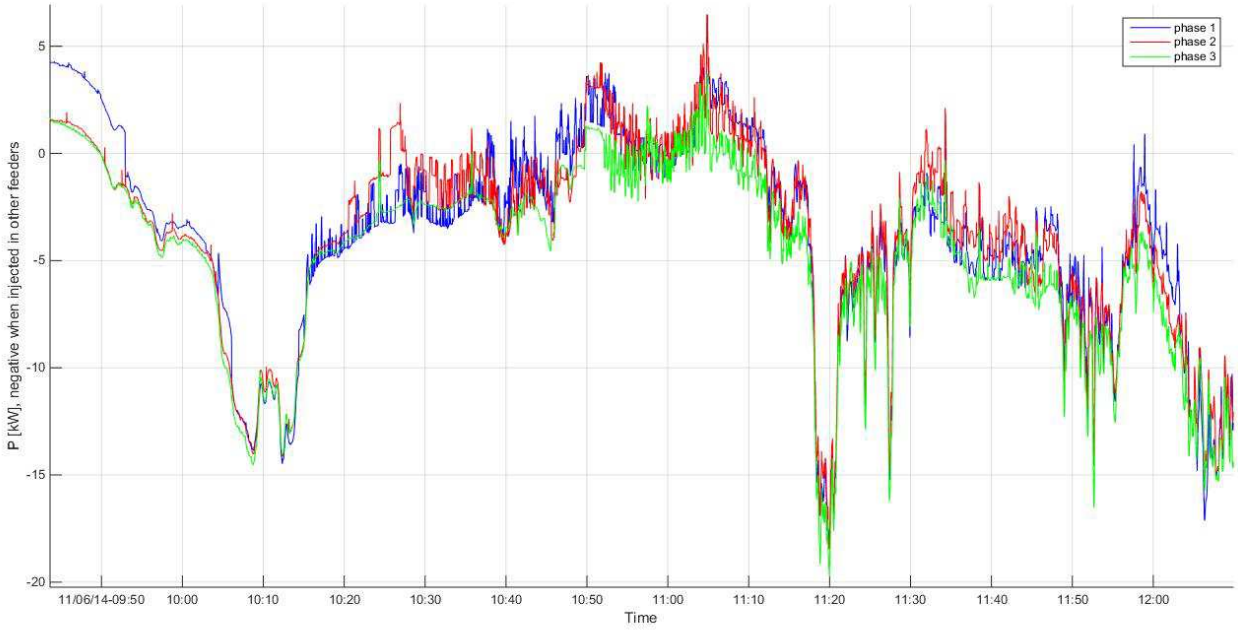

Figure 25: Active power consumption measured at the transformer end of the feeder

3.3.5 Skarpness

Voltage dips and high levels of THD have been observed, whose cause is thought to be the construction equipment rather than distributed energy resources. High levels of power are also occasionally drawn by the zero-energy house and can cause problems, which emphasises the difference energy and power in grid management. Maximum values of voltage THD measured on three phases over three months are given in Figure 25 and line to line voltage variations in Figure 25.

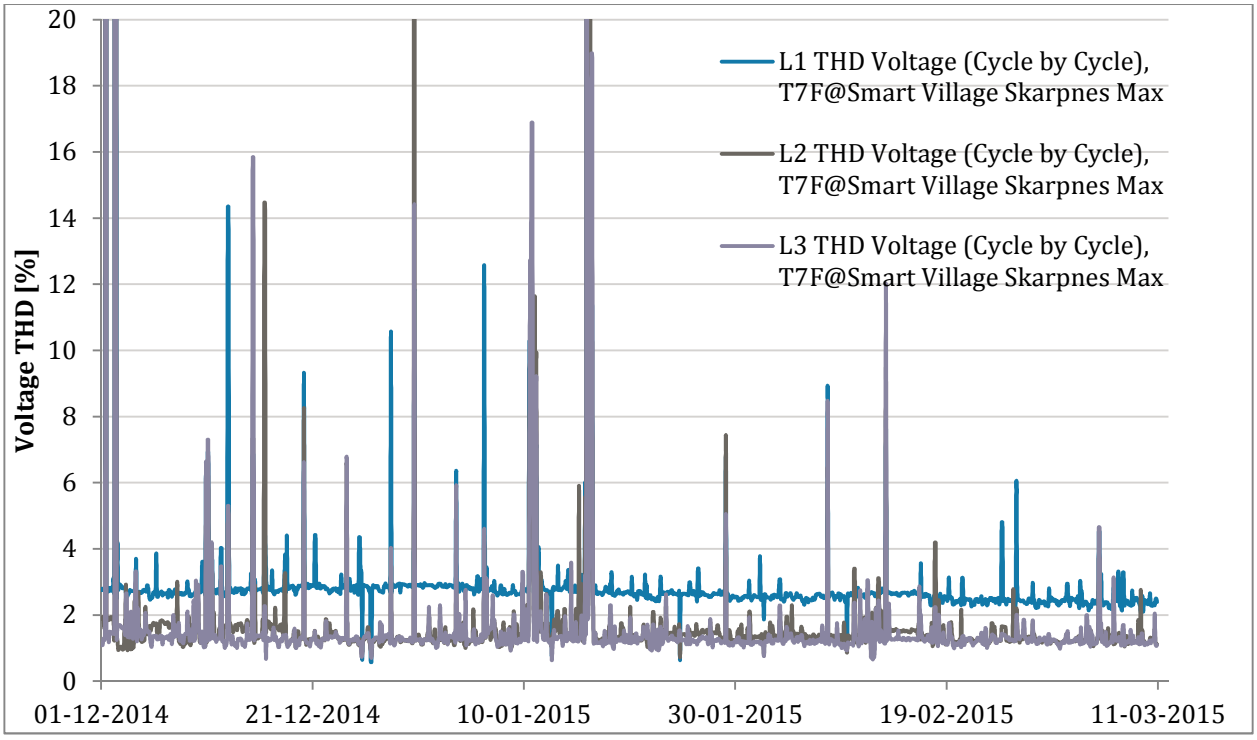

Figure 26: Maximum values of voltage THD measured on three phases over three months (Agder Energi test site)

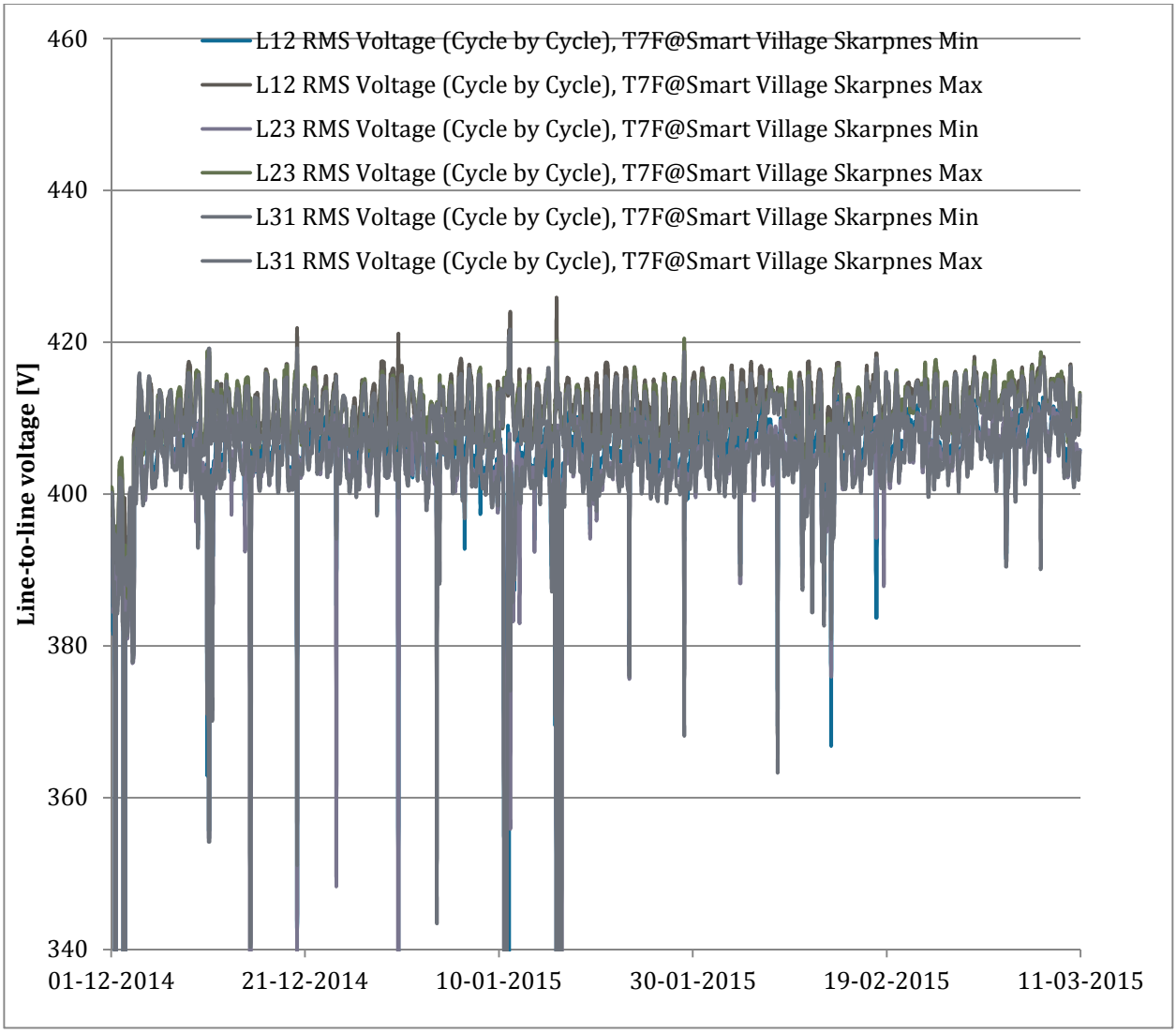

Figure 27: Line-to-line voltage on three phases over 100 days (Agder Energi test site)

4 Impact of the SEMIAH concept on quality of supply

4.1 Possible improvements brought by SEMIAH

Voltage quality issues related to harmonics and power factor are attributed to hardware design and low-level control of the inverters which interface PV systems with the grid. Since the SEMIAH concept has no influence on these aspects of PV generation, no improvements on these aspects of voltage quality can be expected.

The well-documented overvoltage issue due to distributed power generation (cf. paragraph 2.3.1.1) has not been observed in our measurement campaigns since the dimensioning of the investigated feeders had taken into account this risk. However, reverse power flows from one feeder to the others on the LV side of the same transformer routinely occur even in winter. More problematic reverse power flows from the LV to the MV side of the transformer are expected in summer.

Both overvoltage and reverse power flows come from the same fundamental issue i.e., mismatch between local consumption and local production. For voltage issues, the relevant scale is the individual building behind the supply point. Since the first optimisation level in the SEMIAH concept is the single building, the concept has the technical potential to mitigate this issue by guaranteeing temporal alignment between generation and production. This alignment may however conflict with the high-level objectives of the SEMIAH controller: for example, if local PV production is high but production from variable renewables over the balancing area is low, local consumption would need to be reduced to satisfy the high-level objectives and to be increased to prevent local issues. The compromise between these two objectives will depend on regulation for grid connection of distributed generation and on financial incentives and penalties related to voltage quality. Since these parameters are defined by the distribution system operator and may depend on the individual situation of the building, they should be part of the users' preference function for building-level optimisation.

For reverse power flows, the relevant scale is the LV side of each transformer. This is where the intermediate aggregation level foreseen in the SEMIAH controller starts playing a role. Indeed, whereas for voltage control each building has to be controlled, in this case the flexibility of all users on the LV side of a given transformer can be used to prevent reverse power flows. For example, the consumption of non-producing buildings can be shifted to times when their neighbour, power producing buildings generate in excess of their own consumption. This multi-agent optimisation is probably where SEMIAH has the best potential to improve voltage quality in a context of increased penetration of distributed energy generation. In addition to the technical issues described in 2.3.1.7, such a local aggregation would also contribute to reducing grid losses. However, monetising this service will require explicitly including the distribution system operators in SEMIAH's business model.

4.2 Possible detrimental effects

The literature analysis on 2.3.2 has shown that implementation of the SEMIAH concept risks deteriorating voltage quality and grid stability through loss of diversity and rapid voltage fluctuations. Before implementation, loss of diversity and the corresponding impact on line and transformer loading can only be quantified by modelling, some of which is under way in SEMIAH's task 5.6. As household-level optimisation under constraint of users' comfort is at the core of the SEMIAH concept, it is possible that diversity will be maintained without explicit integration in the optimiser.

Rapid voltage variations due to simultaneous switching of controlled appliances will depend on the characteristics of each line where the controller is implemented. A first indication can be obtained from our measurement campaign: an 80 kW difference in power output by the PV power plant (i.e., 55% of its nominal capacity) on the EnAlpin test site translates into a 4% variation in local voltage. Rapid variations of that amplitude would fall under the restrictions set for example by Norwegian regulations. As a first, crude approximation one could therefore estimate that no more than 50% of

the total load on any given feeder should be simultaneously switched to stay within acceptable limits of rapid voltage variations.

4.3 Integration of grid constraints in the SEMIAH concept

Measurements available in SEMIAH are expected to be only energy consumption in participating buildings. This information is an approximate of average active power consumption. It can only provide a crude estimate of the voltage, even if the topology of the network is known, as on low-voltage networks the voltage also depends on reactive power. However, it can provide a good estimate of the coincidence factor. In countries where smart meters can provide local voltage readings (e.g., France, Italy, Latvia, or The Netherlands [2]) using this information would improve the capability of the SEMIAH system to integrate grid constraints.

The power ratings of the lines and transformers and the topology of the network serving each participant should be known if the impact on voltage quality is to be explicitly calculated in the SEMIAH controller. With this approach it would be possible to make the fullest use of all available capacity. However, it requires the active participation of distribution system operators in the deployment of the system. If participation in the SEMIAH concept is to be sold directly to end users by the aggregators, then the impact on voltage quality can only be estimated based on design rules used in the location under consideration, which bears large uncertainties.

With the information available to the SEMIAH controller, maintaining diversity is relatively easy from a computational point of view. The main question is the upper limit under which to keep the coincidence factor, which depends on local design assumptions. However this constraint could limit the flexibility that is effectively available to the system. To minimise this limitation, geographic spread must be maximised when deploying SEMIAH rather than rolling it out to district by district.

5 Conclusion

Two months of power quality measurements have been acquired on two low-voltage feeders, one in Norway and one in Switzerland. These feeders were selected for their high level of distributed PV generation. Thanks to adequate cable sizing, voltage levels remained below upper statutory limits. In general, however, literature shows that overvoltage is likely to be the first issue experienced in most distribution networks with high penetration of distributed energy generation. Observed voltage quality issues in our sites that could be attributed to distributed generation are power factor fluctuations and reverse power flows.

Implementing the SEMIAH concept has the potential to improve the situation with respect to overvoltage and reverse power flows. The former requires optimisation at the single-building level, the latter at the feeder level. The SEMIAH concept however may also degrade voltage quality and grid stability due to loss of diversity, which increases loading of cables and transformers, and due to rapid fluctuations in power consumption leading to rapid voltage changes.

Effectively using the improvement potential from the SEMIAH concept and minimising its potentially negative impact require an intermediate step in the SEMIAH controller at the level of the MV/LV transformer. The precise shape that this intermediate step will take will depend on the information available to it in terms of voltage, power and grid topology, and on the chosen business model. In particular, whether distribution system operators are part or not of the rollout of the SEMIAH concept will define how grid constraints are taken into account.

6 References

[1] P.-J. Alet, “PV integration in the building: drivers, status and challenges,” presented at the Building on PV potential: Turning our walls and rooftops into the building blocks of tomorrow’s energy system, Brussels, Belgium, 26-Jun-2014.

[2] CEER, “5th CEER Benchmarking Report on the Quality of Electricity Supply,” Council of European Energy Regulators (CEER), Brussels, C11-EQS-47-03, Dec. 2011.

[3] CEER, “4th Benchmarking Report on Quality of Electricity Supply,” Council of European Energy Regulators (CEER), Brussels, C08-EQS-24-04, Dec. 2008.

[4] Commission fédérale de l’électricité ElCom, “Qualité de l’approvisionnement en électricité en 2013: Analyse des coupures de courant relevées par l’ElCom,” Commission fédérale de l’électricité ElCom, Bern, 923-12-005, Sep. 2014.

[5] Ofcom, “UK fixed-line broadband performance, November 2014,” Ofcom, Research report, Feb. 2015.

[6] A. Klajn and M. Bątkiewicz-Pantuła, “Standard EN 50160: Voltage characteristics of electricity supplied by public electricity networks,” European Copper Institute, Application Note Cu0147, Mar. 2013.

[7] Verband der Elektrizitätsunternehmen Österreichs (VEO), Verband der Netzbetreiber (VDN), Verband Schweizerischer Elektrizitätsunternehmen (VSE/AES), and České Sdružení Regulovaných Elektroenergetických Spole Čností (CSRES), “Kompendium Technische Regeln zur Beurteilung von Netzrückwirkungen,” VDE, Frankfurt am Main, Germany, 2. Ausgabe, 2007.

[8] Ricerca sul Sistema Energetico - RSE SpA, “Monitoraggio della Qualità della Tensione della Rete di Distribuzione in MT,” *QUEEN: Qualità dell’Energia Elettrica*, 2013. [Online]. Available: http://queen.rse-web.it/home.aspx. [Accessed: 17-Mar-2015].

[9] J. Smith, M. Rylander, and C. Trueblood, “PV Hosting Capacity in Electric Distribution: Monitoring and Feeder Analysis Results from the US,” presented at the 5th International Conference on Integration of Renewable and Distributed Energy Resources, Berlin, Germany, 04-Dec-2012.

[10] C. Bucher, G. Andersson, and L. Küng, “Increasing the PV Hosting Capacity of Distribution Power Grids – A Comparison of Seven Methods,” presented at the 28th European Photovoltaic Solar Energy Conference and Exhibition, Paris, France, 2013, pp. 4231 – 4235.

[11] M. Rekinger, I.-T. Theologitis, G. Masson, M. Latour, D. Biancardi, A. Roesch, G. Concas, and P. Basso, “Connecting the sun: solar photovoltaics on the road to large-scale grid integration,” European Photovoltaic Industry Association, Brussels, Belgium, Full report, Sep. 2012.

[12] T. Stetz, M. Kraiczy, K. Diwold, M. Braun, B. Bletterie, C. Mayr, R. Bründlinger, B. Noone, A. Bruce, I. MacGill, B. Mather, K. Ogimoto, K. Washihara, A. Iaria, A. Gatti, D. Cirio, M. Rekinger, I. T. Theologitis, K. de Brabandere, S. Tselepis, C. Bucher, and Y. Wang, “High Penetration PV in Local Distribution Grids - Outcomes of the IEA PVPS Task 14 Subtask 2,” presented at the EU PVSEC 2014, Amsterdam, 25-Sep-2014.

[13] T. Stetz, M. Rekinger, and I. Theologitis, “Transition from Uni-Directional to Bi-Directional Distribution Grids: Management Summary of IEA Task 14 Subtask 2 — Recommendations

based on Global Experience," International Energy Agency, IEA PVPS T14-03:2014, Sep. 2014.

[14] A. Berger, M. Hennig, and C. Körner, "Voltage control in smart distribution grids-overview and practical experience of available solutions," presented at the 22nd International Conference on Electricity Distribution, Stockholm, Sweden, 2013.

[15] D. Geibel, T. Degner, A. Seibel, T. Bolo, C. Tschendel, M. Pfalzgraf, K. Boldt, P. Muller, F. Sutter, and T. Hug, "Active, intelligent low voltage networks-concept, realisation and field test results," presented at the 22nd International Conference on Electricity Distribution, Stockholm, Sweden, 2013.

[16] A. Navarro, P. Mancarella, L. F. Ochoa, and D. Randles, "Impacts of photovoltaics on low voltage networks: A case study for the North West of England," presented at the 22nd International Conference and Exhibition on Electricity Distribution (CIRED 2013), Stockholm, Sweden, 2013.

[17] Z. Wang, M. Xia, and M. Lemmon, "Voltage stability of weak power distribution networks with inverter connected sources," in *2013 American Control Conference (ACC)*, Washington, DC, 2013, pp. 6577–6582.

[18] M. Hummon, A. Weekley, K. Searight, and K. Clark, "Downscaling Solar Power Output to 4-Seconds for Use in Integration Studies," presented at the 3rd International Workshop on Integration of Solar Power into Power Systems, London, UK, 2013.

[19] R. K. Varma, J. Berge, I. Axente, V. Sharma, and K. Walsh, "Determination of maximum PV solar system connectivity in a utility distribution feeder," presented at the 2012 IEEE PES Transmission and Distribution Conference and Exposition (T&D), Orlando, FL, 2012, pp. 1–8.

[20] P. Wright, G. Murphy, K. Lennon, and P. Clarkson, "Measurements of power quality and voltage level effects associated with a photo voltaic cluster on a domestic housing estate.," presented at the 22nd International Conference on Electricity Distribution, Stockholm, Sweden, 2013.

[21] Y. T. Tan, "Impact on the power system with a large penetration of photovoltaic generation," PhD thesis, The University of Manchester Institute of Science and Technology, Manchester, UK, 2004.

[22] E. de Jaeger, A. du Bois, and B. Martin, "Hosting capacity of LV distribution grids for small distributed generation units, referring to voltage level and unbalance," presented at the 22nd International Conference on Electricity Distribution, Stockholm, Sweden, 2013.

[23] F. Katiraei and J. R. Agüero, "Solar PV Integration Challenges," *IEEE Power Energy Mag.*, vol. 9, no. 3, pp. 62–71, May 2011.

[24] M. M. Aly, M. Abdel-Akher, Z. Ziadi, and T. Senjyu, "Voltage stability assessment of photovoltaic energy systems with voltage control capabilities," presented at the 2012 International Conference on Renewable Energy Research and Applications (ICRERA), Nagasaki, 2012, pp. 1–6.

[25] L. Y. C. Amarasinghe, U. D. Annakkage, and R. A. S. Ranatunga, "A Reactive Power Model for a Simultaneous Real and Reactive Power Dispatch," presented at the 2007 IEEE Power Engineering Society General Meeting, Tampa, FL, USA, 2007.

[26] E. Billette de Villemeur and C. F. Mugombozi, “Pricing reactive power: Some challenges,” presented at the 6th International Conference on the European Energy Market (EEM 2009), Leuven, Belgium, 2009, pp. 1–6.

[27] Commission Staff, “Payment for Reactive Power,” Federal Energy Regulatory Commission, Washington, DC, Staff Paper AD14-7, Apr. 2014.

[28] N. Nibbio, A. Kneuss, P. Chollet, and H. Sauvain, “Impact de la production décentralisée sur les réseaux de distribution,” *Bulletin SEV/AES*, vol. 101, pp. 51–55, 06-May-2010.

[29] Swissgrid SA, “Concept de maintien de la tension dans le réseau de transport suisse à partir de 2011,” Swissgrid SA, Frick, Switzerland, Apr. 2010.

[30] L. M. Cipcigan and P. C. Taylor, “Investigation of the reverse power flow requirements of high penetrations of small-scale embedded generation,” *IET Renew. Power Gener.*, vol. 1, no. 3, pp. 160–166, Sep. 2007.

[31] G. Bianco, L. Consiglio, G. Di Lembo, G. Sapienza, and G. Valvo, “Unwanted island maintaining in LV grids: analysis and possible solutions. A study based on the real-time digital simulator,” presented at the 22nd International conference on Electricity Distribution, Stockholm, Sweden, 2013.

[32] V. Bufano, C. D’Adamo, L. D’Orazio, and C. D’Orinzi, “Innovative solutions to control unintentional islanding on LV network with high penetration of distributed generation,” presented at the 22nd International conference on Electricity Distribution, Stockholm, Sweden, 2013.

[33] P. Suwanapingkarl, “Power quality analysis of future power networks,” PhD thesis, Northumbria University, Newcastle, 2012.

[34] S. Rönnberg, M. Bollen, and A. Larsson, “Grid impact from PV-installations in northern Scandinavia,” presented at the 22nd International conference on Electricity Distribution, Stockholm, Sweden, 2013.

[35] M. Klatt, J. Meyer, P. Schnegner, A. Koch, J. Myrzik, C. Körner, T. Darda, and G. Eberl, “Emission levels above 2 kHz-laboratory results and survey measurements in public low voltage grids,” presented at the 22nd International conference on Electricity Distribution, Stockholm, Sweden, 2013.

[36] M. Roozbehani, M. A. Dahleh, and S. K. Mitter, “Volatility of Power Grids Under Real-Time Pricing,” *IEEE Trans. Power Syst.*, vol. 27, no. 4, pp. 1926–1940, Nov. 2012.

[37] J. L. Mathieu, T. Haring, J. O. Ledyard, and G. Andersson, “Residential Demand Response program design: Engineering and economic perspectives,” presented at the 10th International Conference on the European Energy Market (EEM 2013), Stockholm, Sweden, 2013, pp. 1–8.

[38] M. Orphelin and J. Adnot, “Improvement of methods for reconstructing water heating aggregated load curves and evaluating demand-side control benefits,” *IEEE Trans. Power Syst.*, vol. 14, no. 4, pp. 1549–1555, Nov. 1999.

[39] O. Krone, “Netzstabilisierung und smartRSA,” presented at the Bauholzmesse, Bern, Switzerland, 14-Nov-2014.

[40] M. Orphelin, “Modélisation par chaînes de Markov homogènes ergodiques des appels de puissance d’un parc de chauffe-eau électriques.,” *MODULAD*, no. 25, Jun. 2000.

[41] W. Zhang, K. Kalsi, J. Fuller, M. Elizondo, and D. Chassin, “Aggregate model for heterogeneous thermostatically controlled loads with demand response,” in *2012 IEEE Power and Energy Society General Meeting*, San Diego, CA, USA, 2012.

[42] E. Agneholm, “Cold Load Pick-up,” Doctoral thesis, Chalmers University of Technology, 1999.

[43] J. W. Black and R. Tyagi, “Potential problems with large scale differential pricing programs,” in *2010 IEEE PES Transmission and Distribution Conference and Exposition*, New Orleans, USA, 2010.

[44] N. Pigenet, “Mise en place des outils de suivi et de prédiction de la demande électrique à l’échelle d’un territoir, application au département du Lot,” Université Toulouse III - Paul Sabatier, Toulouse, France, 2009.

[45] D. Da Silva, “Analyse de la flexibilité des usages électriques résidentiels : application aux usages thermiques,” PhD thesis, École Nationale Supérieure des Mines de Paris, Paris, France, 2011.

[46] F. A. M. Rizk and G. N. Trinh, *High Voltage Engineering*. Boca Raton, FL: CRC Press, 2014.

[47] D. Craciun and D. Geibel, “Evaluation of ancillary services provision capabilities from distributed energy supply,” presented at the 22nd International conference on Electricity Distribution, Stockholm, Sweden, 2013.

[48] G. Conte, *Impianti Elettrici 1*, 3rd ed. Milano, Italy: Ulrico Hoepli Editore, 1996.

[49] Elspec, “Blackbox: G4K Fixed PQ Analyser,” Elspec, Datasheet SMX-1108-0100, Oct. 2013.

[50] HAAG, “Euro-Quant: Das erste Messgerät für den rückführbaren Vergleich der Netzqualität an allen Messstellen Europas,” HAAG Elektronische Messgeräte GmbH, Waldbrunn, Brochure.

[51] J. Pargätzi, “Omni-Quant: Quick Start,” Parmeltec Mess- und Elektrotechnik GmbH, Lüen, May 2014.

[52] University of California, San Diego, “Improving economics of solar power through resource analysis, forecasting, and dynamic system modeling,” California Public Utilities Commission, San Francisco, CA, USA, Final Project Report, Nov. 2013.

[53] A. Toliyat, A. Kwasinski, and F. M. Uriarte, “Effects of high penetration levels of residential photovoltaic generation: Observations from field data,” in *2012 International Conference on Renewable Energy Research and Applications (ICRERA)*, Nagasaki, 2012.

7 Change History

Revision	Date	Responsible	Comment
0.5	2015-03-23	Pierre-Jean Alet	First version. Submitted for 1RP.
1.0	2015-07-07	Pierre-Jean Alet	Updated in accordance with comments from the Technical Review Report: - Text in Section 2.3.3 has been updated to clarify the concent of Table 3. - Minor editorial corrections.